NEW RESEARCH ON NEURONAL NETWORKS

NEW RESEARCH ON NEURONAL NETWORKS

MOMOKA YOSHIDA
AND
HARUKA SATO
EDITORS

Nova Science Publishers, Inc.
New York

LIBRARY OF CONGRESS CATALOGING-IN-PUBLICATION DATA

New research on neuronal networks/Momoka Yoshida and Haruka Sato(editors).
p. cm.
Includes bibliographical references and index.
ISBN 978-1-60456-561-4(hardcover)
1. Neural networks(Neurobiology) I.Yoshida,Momoka.II.Sato,Haruka.
[DNLM:1.Nerve Net.WL 102 N5317 2008]
QP363.3N59 2008
612.8'5—dc22

2008012764

Published by Nova Science Publishers, Inc. ✣ New York

CONTENTS

PREFACE

In outline, a neural network describes a population of physically interconnected neurons or a group of disparate neurons whose inputs or signalling targets define a recognizable circuit. Communication between neurons often involves an electrochemical process. The interface through which they interact with surrounding neurons usually consists of several dendrites (input connections), which are connected via synapses to other neurons, and one axon (output connection). If the sum of the input signals surpasses a certain threshold, the neuron sends an action potential (AP) at the axon hillock and transmits this electrical signal along the axon. This book presents important new research in this field.

Chapter 1 - The mammalian olfactory bulb (OB) is a specialized part of the brain, receiving sensory input from the nasal olfactory epithelium. The olfactory glomeruli are spheroid-like structures (~100 μm in diameter) thought to represent "unitary" coding modules in central olfactory processing. Each glomerulus may be considered a structural and functional unit for processing sensory input, because each one is formed by a set of functionally and morphologically stereotyped juxtaglomerular neurons, specifically organized to perform discrete network operations. Each glomerulus also comprises dendrites of a set of mitral and tufted cells, the output neurons of the OB. Importantly, all intraglomerular synaptic interactions are dendrodendritic. This arrangement shapes the input-output transfer of olfactory information. As glomeruli have the same neural content, each glomerulus is a discrete ensemble or network module consisting of sensory afferents, interneurons and output cells.

There are three types of juxtaglomerular interneurons: glutamatergic external tufted (ET), GABAergic periglomerular (PG) and glutamatergic short axon (SA) cells with characteristic morphological and physiological features. ET cells have intrinsic, rhythmic burst firing and are contacted directly by olfactory nerve terminals. ET cells of the same glomerulus fire in synchrony and directly elicit bursts of EPSPs in PG and SA cells, most of which do not receive olfactory nerve input. The ensemble of synchronously bursting ET cell can monosynaptically synchronize activity of other neurons within the same glomerulus, and may possibly coordinate activity of mitral cells via glutamate spillover. Periglomerular cell dendrites ramify in a restricted portion of a single glomerulus and thus might serve for local intra-glomerular inhibition via dendrodendritic interactions with ET or mitral cell dendrites. By contrast, SA cell dendrites do not ramify in glomeruli, instead dendrites and axons of short-axon cells propagate throughout several glomeruli within the glomerular layer and thus might serve for inter-glomerular communication. The interglomerular cross-talk provides, on

the one hand, lateral inhibition upon arrival of a strong sensory input, or on the other hand, recruitment of a group of modules into cooperative activity. Interplay among individual modules suggests that the glomerular layer is not a set of isolated structural units, but may play a role of a specific subsystem in the OB, performing an initial analysis of odor information. This subsystem may compute intensity of odors and provide this information to downstream circuits for further computation. The olfactory bulb is an attractive model to study the cellular mechanisms underlying the encoding, transfer, processing and decoding of sensory information.

Chapter 2 - Perhaps the first to study detection of signals under conditions of variability and ambiguity was Fechner, the founder of psychophysics, when using simple perceptual experiments and mathematics he attempted to find relations between human internal (mental) and external (physical) worlds. In the early 20^{th} century, the explosive development of radio and electric/electronic communication technologies provided a strong impetus to intensively research signal processing problems by strict methods of physics and mathematics. Sampling, or Shannon-Kotelnikov theorem for band-limited signals, information, and the theory of optimum noise immunity became the milestones for this field and initiated its flourishing when the theory was elaborated and applied successfully to solving numerous extremely important problems in science and technology. Once signal detection/processing theory matured, it was turned to psychology where it has already attained many outstanding achievements.

Chapter 3 - Computational Neuroscience provides tools to abstract and generalize principles of brain function using mathematics, with applicability to the entire neuroscience spectrum including molecular, cellular, systems, and translational levels (NIH Neuroscience Blueprint 2004). Researchers are investigating brain organization at specific levels of scale, ranging from molecular to behavioral levels, each of which provides important insights into the specific sub-system. However, improved understanding of the functional organization typically requires connection of multiple levels, something that can be facilitated by computational models. For instance, recent technical advances have resulted in a rapid accumulation of information on intracellular signaling pathways and relationships to long-term neuronal changes. Computational techniques and tools are being developed to model such mechanisms with increasing accuracy and are found to be essential to generate an understanding of the underlying functions in this case. Indeed, computational models based on the real anatomy and physiology of the nervous system already constitute what is, in effect, a compact and self-correcting database of neurobiological facts and functional relationships. There is increasing belief that laboratories and researchers will rely on models and modeling software to check the significance and accuracy of their data, and that these models will enhance collaboration and communication within neuroscience.

The best computational work is both informed by and subsequently contributes to a biological understanding of the nervous system. As cited, one of the reasons computational approaches to questions about the nervous system have the potential to be so valuable is that these approaches span the spectrum of neuroscience from molecular to behavioral levels. Computational approaches also allow us to fine tune hypotheses before testing them in biological systems, streamlining the discovery process and decreasing the volume of the use of animal models. Therefore, computational neuroscientists and biological neuroscientists are interdependent groups – neither can reach the full capabilities of their work without the other. This chapter reviews principles of computational modeling in brain circuits (section 2) and

illustrates the utility of computational approaches in the case of neuroplasticity due to cocaine in the glutamatergic pathway from the prefrontal cortex (PFC) to the nucleus accumbens (NAc) (section 3).

Chapter 4 - Auditory evoked potential (AEP) in the rat auditory cortex has typical fast positive/negative biphasic onset waves (P1/N1), referred to as middle latency responses (MLRs), and slow biphasic waves (P2/N2), referred to as long latency responses (LLRs), which together form the P1-N1-P2-N2 complex and is occasionally associated by relatively fast biphasic offset responses (POFF/NOFF). The authors review their recent studies that investigated MLRs, LLRs and offset responses by multiple-site surface microelectrode recording. The surface microelectrode array had 10 by 7 recording points in a 3.5-mm by 3-mm area that covered the majority of the auditory cortex including the primary, anterior, and ventral auditory fields (AI, AAF and VAF). Tone bursts served as test stimuli. MLRs in each of the auditory fields showed a different place code of intensity and frequency, and specifically had a different manner of intensity coding that altered with steady and dynamic states of sound intensity. The temporal structure of AEP, i.e., a combination of MLR and LLR amplitudes at an arbitrary location, could also distinguish the steady and dynamic states. The offset responses also depended on steady and dynamic states of sound with a complementary frequency-tuning characteristic to the onset MLR. Thus, sound information is distributed spatially and temporally in various aspects in the auditory cortical representation.

Chapter 5 - The premotor areas are defined as areas of the frontal cortex that share connections with the primary motor area, contain separate representations of distal musculature and are sites of origin for corticospinal projections. Although extensive research has been conducted in premotor areas over the last few decades, their respective roles in motor control are still incompletely understood. In this chapter, the author focuses on the ventral premotor cortex (PMv), an area that has been extensively studied in squirrel monkeys. PMv is a motor area that exclusively contains forelimb and orofacial representations. It is believed to be a unique specialization of primate species that exist in all primates, but in no other mammals. The author and colleagues recently have documented the pattern of connectivity of PMv in squirrel monkeys and found consistency with what has been described in other primates. It thus appears that PMv's intracortical network is conserved across species, which is suggestive that its function is also preserved. In this chapter, the author first provides a general overview of the premotor areas and the literature on the specific role of the PMv in motor control. Because the anatomical network of a given area provides a solid framework to guide hypothetical constructs of its function, he then reviews the pattern of connections of PMv found across primate species and provide information on the role of the diverse areas sharing connections with PMv.

Chapter 6 - Computationally effective inverse analysis algorithms are crucial for damage detection and parametric identification, reliability and performance evaluation and control design of real dynamic structural systems. Soft structural parametric identification strategies for structural health monitoring (SHM) with neural networks by the direct use of forced vibration displacement, velocity or free vibration acceleration measurements without any frequencies and/or mode shapes extraction from measurements are proposed. Two three-layer back-propagation neural networks, an emulator neural network (ENN) and a parametric evaluation neural network (PENN), are constructed to facilitate the identification process. The rationality of the proposed methodologies is explained and the theoretical basis for the construction of the ENN and PENN are described according to the discrete time solution of

structural vibration state space equation. The accuracy and efficacy of the proposed strategies are examined by numerical simulations. The performance of the free vibration measurement based methodology under different initial conditions and the efficiency of neural networks with different architecture are also discussed. The effect of measurement noises on the performance of the forced vibration dynamic responses based parametric identification methodology is investigated and a noise-injection method is introduced to improve the identification accuracy. Since the strategy does not require the extraction of structural dynamic characteristics such as frequencies and mode shapes, it is shown computationally efficient. Unlike any conventional system identification technique that involves the inverse analysis with an optimization process, the proposed strategies in this chapter can give the identification results in a substantially faster way and can be viable tools for near real-time identification of civil infrastructures instrumented with monitoring system.

Chapter 7 – The authors present a review of their computer algorithms developed for the shape detection technique. The study of this chapter involves the laser line projection technique, image processing and approximation neural networks. To extract topographic information of the shape of an object, it is scanned by means of a laser line. From the scanning procedure, a set of images is captured by a CCD camera. By processing these images, the object shape is recovered. The shape information is extracted from an image by detecting the behaviour of the position of the laser line in the image plane. To determine the mathematical model of the relationship between the laser line behaviour and the object shape, approximation neural networks are applied. Approximation networks such as Radial Basis Function neural networks, General Regression neural networks and Bezier neural networks are used to create a model of the behaviour of the laser line. The architecture of these approximation networks is built using data of images of a laser line projected on objects, whose dimensions are known. The data correspond to the object dimensions of the region where the laser line is projected. In this manner, the approximation network is constructed. The approach of the approximation networks in this technique is the calibration procedure of shape detection by computer algorithms. In this form, the accuracy of the shape measurements is improved. It is because errors of parameters measured on the set-up are not introduced to the system. The results of this examination are presented by computer simulation and in experimental form.

Chapter 8 - One of the basic differences between the brain and the computer is composition. The computer comprises electrical switches that can function only in an elementary manner. In contrast, the neuron, which is a component of the brain, is a considerably complicated structure. Although neuron is represented as a single nonlinear element, or just a single 'point' schematically, in the classical notion of neural networks, actual neurons in the brain typically have widely extended and branched dendrites with a number of nonlinear processes. A lot of experimental and modelling studies have been exploring potential computational ability of the dendrite, revealing several possible ways in which single neurons could function in an intelligent manner under the favour of their dendrites. Since the neuron is a component of the neuronal network and thus usually does not work alone but cooperate with other neurons in the network, a subsequent question is what impact such dendritic computation could have on the performance of the entire network. It would be natural to assume that if the component, the neuron, can function intelligently by virtue of the dendrite, it would automatically contribute to the intelligence of the system to which it belongs. However, it is actually a huge challenge to elucidate exactly how the

dendritic biophysical mechanisms cooperate with the network structures to execute actual specific computations operated in the brain. In this chapter, the author introduces several recent modelling studies, with some focus on his group's own research, that try to clarify the functional roles of the dendrite in the entire neuronal network, which executes specific neurocognitive functions such as short-term memory or pattern discrimination.

Chapter 9 - The understanding of brain function is one of the major challenges facing natural science these days. As a very complex system, the brain is attracting the attention not only of neurophysiologists, but also of physics-oriented minds working in the fields of complexity and dynamical systems theory. Complexity at almost all levels, from the individual brain cell to the neuronal circuitry, invites the application of conceptual frameworks and methodologies used in these fields; and yet, the normal practice in brain research concentrates on very precise, highly averaged results and data presentation, carefully avoiding traces of variability and fluctuations. However, it is precisely the omnipresent, fluctuating patterns of activity at all levels of nervous system function, that exemplify and represent the essence of brain function and its relation to behaviour. The authors' paper is an attempt to provide an overview of some current approaches to the study of noise, fluctuations and variability in neuroscience, and to concentrate upon fluctuations in coordinated activity in the brain, represented by synchronization of neuronal activity in electrophysiological recordings. Careful consideration of the synchronization and desynchronization patterns in brain networks will yield crucial information to unravel brain dynamics and relate it to the behaviour of the organisms. In general, the scrutiny of variability and fluctuations in neuronal activity will complement recent studies that attribute, rather than stable, metastable states to brain function, and will illuminate the relation between brain complexity and purposeful behaviour.

In: New Research on Neuronal Networks
Editor: M. Yoshida and H.Sato
ISBN 978-1-60456-561-4

Chapter 1

NEURONAL MODULES OF THE OLFACTORY BULB

S. V. Karnup[1,2] and A. Hayar[3]
[1] University of Maryland School of Medicine, Baltimore, MD 21201,
[2] Institute of Theoretical and Experimental Biophysics,
Pushchino, 142292, Russia,
[3] University of Arkansas for Medical Sciences,
Little Rock, AR 72205

The mammalian olfactory bulb (OB) is a specialized part of the brain, receiving sensory input from the nasal olfactory epithelium. The olfactory glomeruli are spheroid-like structures (~100 μm in diameter) thought to represent "unitary" coding modules in central olfactory processing. Each glomerulus may be considered a structural and functional unit for processing sensory input, because each one is formed by a set of functionally and morphologically stereotyped juxtaglomerular neurons, specifically organized to perform discrete network operations. Each glomerulus also comprises dendrites of a set of mitral and tufted cells, the output neurons of the OB. Importantly, all intraglomerular synaptic interactions are dendrodendritic. This arrangement shapes the input-output transfer of olfactory information. As glomeruli have the same neural content, each glomerulus is a discrete ensemble or network module consisting of sensory afferents, interneurons and output cells.

There are three types of juxtaglomerular interneurons: glutamatergic external tufted (ET), GABAergic periglomerular (PG) and glutamatergic short axon (SA) cells with characteristic morphological and physiological features. ET cells have intrinsic, rhythmic burst firing and are contacted directly by olfactory nerve terminals. ET cells of the same glomerulus fire in synchrony and directly elicit bursts of EPSPs in PG and SA cells, most of which do not receive olfactory nerve input. The ensemble of synchronously bursting ET cell can monosynaptically synchronize activity of other neurons within the same glomerulus, and may possibly coordinate activity of mitral cells via glutamate spillover. Periglomerular cell dendrites ramify in a restricted portion of a single glomerulus and thus might serve for local intra-glomerular inhibition via dendrodendritic interactions with ET or mitral cell dendrites. By contrast, SA cell dendrites do not ramify in glomeruli, instead dendrites and axons of short-axon cells propagate throughout several glomeruli within the glomerular layer and thus might serve for inter-glomerular communication. The interglomerular cross-talk provides, on

the one hand, lateral inhibition upon arrival of a strong sensory input, or on the other hand, recruitment of a group of modules into cooperative activity. Interplay among individual modules suggests that the glomerular layer is not a set of isolated structural units, but may play a role of a specific subsystem in the OB, performing an initial analysis of odor information. This subsystem may compute intensity of odors and provide this information to downstream circuits for further computation. The olfactory bulb is an attractive model to study the cellular mechanisms underlying the encoding, transfer, processing and decoding of sensory information.

1. INTRODUCTION

The sense of smell is critically important for food consumption, emotional responses, aggression, maternal and reproductive functions, neuroendocrine regulation, and the recognition of conspecifics, predators, and preys. The main olfactory bulb (MOB) is the first brain structure in the olfactory system that processes olfactory signals relayed from olfactory receptor neurons (ORNs) in the nasal epithelium. The olfactory bulb has become an attractive model to study cellular mechanisms underlying the encoding, transfer, processing and decoding of sensory information. Interest in this area was sparked by a series of dramatic breakthroughs over the past decade in our understanding of the organization and function of the peripheral olfactory system, cloning of the olfactory receptors, and identification of the olfactory transduction machinery [reviewed by Breer, 2003]. These advances, together with a wealth of accumulated knowledge about the anatomy and connectivity of the bulb [reviewed by Shipley et al., 1996], have set the stage to unravel the mechanisms of early sensory processing by bulbar circuits.

Olfactory receptor neurons, expressing the same odorant receptor, project onto one or very few glomeruli in each main olfactory bulb, where they terminate on the apical dendrites of mitral/tufted cells and local juxtaglomerular (JG) neurons. The glomeruli, thus, are the initial site of synaptic processing in the olfactory system. Synchronous activity occurs among output mitral cells associated with the same glomerulus [Carlson et al., 2000; Schoppa and Westbrook, 2002]. Such synchrony appears to be of glomerular origin, but its mechanism is still poorly understood. It has been proposed that both electrical and synaptic dendritic interactions could help to establish precise timing relationships among olfactory bulb output neurons [reviewed by Lowe, 2003; Schoppa and Urban, 2003]. Synchronization of olfactory neurons may play an important role in odor discrimination [Stopfer et al., 1997; Linster and Cleland, 2001; reviewed by Laurent et al., 2001]. Neural synchronization is also a fundamental mechanism that facilitates transmission of sensory information from one brain region to another [Alonso et al., 1996; Konig et al., 1996; Roy and Alloway, 2001]. In particular, coincident bursts of action potentials invading the presynaptic terminals could be the most powerful stimulus to excite a postsynaptic neuron [reviewed by Lisman, 1997]. This chapter reviews our current knowledge of olfactory bulb circuitry, and in particular olfactory input processing at the level of the glomeruli.

2. OVERVIEW OF MAIN OLFACTORY BULB CIRCUITRY

Odors are transduced by ORNs, giving rise to action potentials that propagate along the axons of ORNs- the olfactory nerve (ON) fibers. These fibers form bundles, which then

collect as groups of fascicles, pass through the cribriform plate, and establish synapses with neural elements in the glomerular layer (GL).

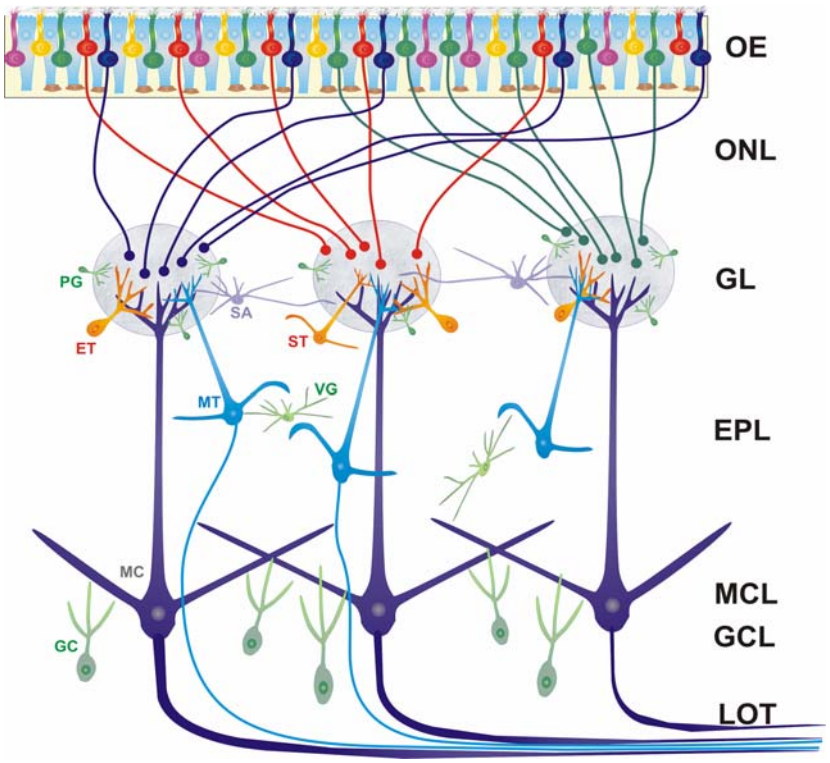

Figure 1. Schematic illustration of the basic circuitry of the MOB including the projections of ORNs from the olfactory epithelium (OE) to the glomerular layer (GL). Note that ORNs expressing different odorant receptor genes (shown as blue, red or green cells) are interspersed and widely distributed, yet the axons of ORN expressing the same odorant receptor gene converge onto the same glomerulus (or pairs of medial and lateral glomeruli) in the GL. Axons of ORNs travel in the ONL and synapse in the GL on the dendrites of mitral cells (MC), superficial and middle tufted cells (ST&MT) and generic juxtaglomerular (JG) neurons, which include periglomerular cells (PG), external tufted cells (ET) and short axon cells (SA). SA cell interconnect different glomeruli. There are serial and reciprocal synapses between the apical dendrites of mitral/tufted cells and the processes of JG neurons within the glomerular neuropil. ST are located in the superficial external plexiform layer (EPL) or at the GL-EPL border. The lateral dendrites of mitral/tufted cells form serial and reciprocal synapses with the apical dendrites of granule cells (GC) in the EPL. The majority of GCs are concentrated in the GC layer (GCL) but a few lie within the MCL. The axons of mitral/tufted cells project locally to GCs (not shown) and also to primary olfactory cortex via the lateral olfactory tract (LOT). The bulb also contains other populations of interneurons neurons, including the van Gehuchten cells (VG) within the EPL.

Based on anatomical considerations (high packing density of unmyelinated axons), and computational modeling studies [Bokil et al., 2001], it has been speculated that ephaptic interactions (current spread through the extracellular space) might synchronize ON fibers. ORNs expressing the same receptor project to one or two glomeruli located on the medial and/or lateral side of each MOB [Figure. 1; Ressler et al., 1993, 1994; Vassar et al., 1994; Mombaerts et al., 1996; Wang et al., 1998; Potter et al., 2001; Treloar et al., 2002].

Studies in transgenic animals showed that this projection pattern is topographically fixed across animals. That is, the same glomeruli identified in different mice receive inputs from the same restricted population of ORNs bearing the same receptor [Mombaerts et al., 1996; Potter et al., 2001; Treloar et al., 2002; Wang et al., 1998]. Rough calculations confirm an

approximately 1:2 ratio between the number of different types of receptors (~1,000) and the total number of glomeruli (~1,800) in mice. ORNs utilize glutamate as their primary neurotransmitter [Sassoè-Pognetto et al., 1993]. In addition, there are a few potential neuromodulators such as carnosine, a soluble dipeptide, and zinc and copper, which are present in high concentrations in mammalian ORNs and ON axon terminals in the GL [Biffo et al., 1990; Ferriero et al., 1975; Margolis, 1980].

The MOB in rodents is situated at the rostral pole of the cranial cavity and it is connected to the frontal cortex by a slender peduncle. The bulb is composed of distinct layers or laminae that are organized as concentric circles on a coronal section. These layers, from superficial to deep, are the ONL, GL, external plexiform layer (EPL), mitral cell layer (MCL), internal plexiform layer (IPL), GC layer (GCL), and the ependymal layer (Figure 1). The ONL consists of ON axons and glial cells [Cajal, 1911a,b; Doucette, 1989; Pinching and Powell, 1971b]. Deep to the ONL, the GL is comprised of neuropil-rich ovoid structures – the glomeruli – each of which is surrounded by a shell of small neurons and glia. Within the glomeruli, ON axons synapse with mitral and tufted cells, as well as with the intrinsic neurons of the GL – the juxtaglomerular (JG) cells. Adjacent glomeruli are somewhat isolated from each other by astrocytes residing in the glomerular shell [Bailey and Shipley, 1993]. The EPL lies beneath the glomeruli, and it primarily consists of dense neuropil formed by the dendrites of mitral cells and granule cells (GCs) that ascend from the MCL and GCL, respectively. The EPL also contains several subtypes of tufted cells and intrinsic interneurons. Nevertheless, the dominant feature of the EPL is the extensive dendrodendritic synapses between mitral/tufted cells and GCs. Deep to the EPL, the MCL is a thin layer that contains the somata of mitral cells, as well as numerous GCs [Cajal, 1911a,b]. Together with tufted cells, mitral cells are the major class of output cells of the bulb. They extend a single apical dendrite into the GL, where it arborizes extensively throughout much of a single glomerulus. The apical dendrites are synaptically contacted by ON terminals [Price and Powell, 1970a; Shepherd, 1972]. The secondary or lateral dendrites of mitral and deep tufted cells ramify in the lower part of EPL where they form dendrodendritic synapses with dendrites of GCs; secondary dendrites of middle tufted cells (somata in the superficial two-thirds of EPL) are shorter and they extend in the superficial half of EPL. Mitral and deep tufted cells project axons to all regions of the olfactory cortex, whereas middle tufted cells project their axons selectively to the rostromedial region of the olfactory cortex [Ekstrand et al., 2001; Haberly and Price, 1977; Mori et al., 1983; Orona et al., 1984; Price and Powell, 1970b; Scott, 1981]. Deep to the MCL, the IPL is the relatively thin layer with a low density of cells. The GCL is the deepest neuronal layer in the bulb, and it contains the largest number of cells. Most of the neurons of the GCL are the GCs, but there are also small numbers of Golgi cells, Cajal cells, and Blanes cells. The GCs are inhibitory GABAergic cells; they do not have axons and establish dendrodendritic synapses with mitral/tufted cells in the EPL.

3. THE GLOMERULUS AS A MODULE FOR OLFACTORY CODING

The olfactory glomeruli are spheroid-like structures (100-120 μm in diameter) thought to represent "unitary" coding modules in central olfactory processing. This concept is supported by the fact that they are the initial site of synaptic integration in the olfactory pathway and they form a spatial map that reflects the activity of olfactory receptor neurons. Olfactory nerve (ON) axons arising from olfactory receptor neurons expressing the same odorant receptor converge onto the same one or few glomeruli in each main olfactory bulb, where

they synaptically terminate on the apical dendrites of mitral/tufted cells and local juxtaglomerular (JG) neurons. Individual odorants elicit specific spatial patterns of glomerular activity, and different odorants activate different patterns of glomeruli [Jourdan et al., 1980; Cinelli et al., 1995; Johnson and Leon, 2000a,b; Belluscio and Katz, 2001].

Each glomerulus may be considered a functional unit for processing sensory input because each one is comprised of a small set of functionally and morphologically stereotyped neuron types, specifically organized to perform discrete network operations. These operations shape the transfer of information from ON terminals to mitral and tufted cells, the output neurons of main olfactory bulb. As all glomeruli have the same compliment of neural elements, each glomerulus unifies sensory afferents, interneurons and output cells in a discrete neural network module. The glomeruli may function to compute the intensity of odors and provide this information to downstream circuits for further computation. Specifically, the glomeruli could prolong and amplify mitral cell responses to odors in a concentration-dependent manner, and they could initiate odor contrast enhancement via interglomerular lateral inhibition as suggested by our recent study [Aungst et al., 2003].

Each glomerulus contains the apical dendritic tufts of about 20 mitral cells, about 200 medium and deep tufted cells and the dendrites of 1500 - 2000 JG cells [Shipley et al., 1996]. Dendrites of all cells contain both presynaptic and postsynaptic sites, i.e. each dendrite can release neurotransmitter and receive a synaptic input. Practically all interactions among neurons of the glomerular module occur in the glomerular core via elaborately interweaved dendrites. Our understanding of the glomerular circuitry is limited and has not changed appreciably since the classical Golgi and electron microscopic studies of Pinching and Powell [1971a,b]. Those studies described at least 3 different populations of JG cells, namely periglomerular (PG), short axon (SA) and external tufted (ET) cells. These 3 cell classes were traditionally thought to be inhibitory interneurons. Our new studies, however, demonstrate that ET and SA cells are excitatory and only PG cells are inhibitory. Recent immunohistochemical and electron microscopic studies indicate that PG cells are heterogeneous in their synaptic connections as well as in their neurochemical and morphological features. PG cells contain GABA and/or dopamine. ON terminals form excitatory glutamatergic synapses with all ET and mitral/tufted cells but only with some PG cells [for review, see Kosaka et al., 1998]. In addition, excitatory and inhibitory cells form reciprocal dendrodendritic synapses in the glomerular neuropil. Thus, synaptic integration in the glomeruli seems to involve a complex neuronal circuitry, the functional organization of which is under intensive investigation.

4. NEUROPHYSIOLOGICAL AND ANATOMICAL PROPERTIES OF JG NEURONS

The neurons of the GL are classified into three cell types, which include (1) periglomerular (PG) cells; (2) external tufted (ET) cells; (3) short axon (SA) cells [Blanes, 1898; Cajal, 1911a,b; Golgi, 1875; Pinching and Powell, 1971a,b,c; Pinching and Powell, 1972b,c; Van Gehuchten and Martin, 1891]. Collectively, the intrinsic neurons of the GL are referred to as juxtaglomerular (JG) cells. The term JG is also used here with regard to cited studies in which the subtype of glomerular neuron was not specified. The morphology of biocytin-filled JG cells is illustrated in Figure 2, Figure 3 and Figure 11 E.

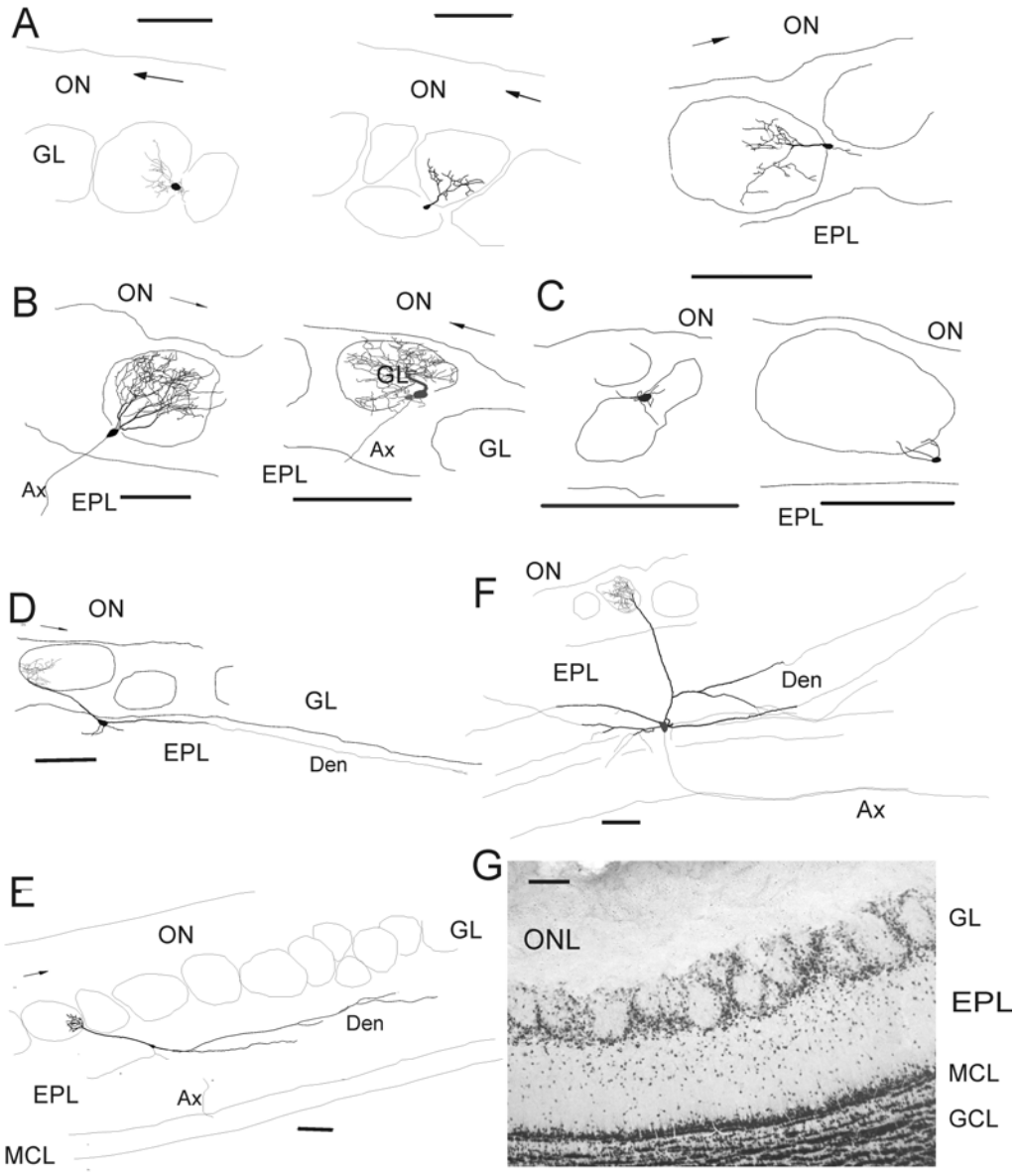

Figure 2. Types of juxtaglomerular cells. *A-F* Reconstruction of biocytin-labeled neurons having their dendritic arborization in a single glomerulus. *A* – three classic periglomerular (CPG) cells with a branching primary dendrite within the glomerulus. *B* – two external tufted (ET) cells with the somata in the glomerular shell and an extensive dendritic tuft occupying an entire glomerulus. *C* – two hairy periglomerular (HPG) cells with hair-like processes. *D* – superficial tufted (ST) cell having a long primary dendrite terminating with a tuft, cell body in the upper EPL and a few long secondary dendrites parallel to GL/EPL border. (*E*) – medium tufted (MT) cell with the soma deep in the EPL. (*F*) – mitral (M) cell with a tufted primary dendrite and long lateral dendrites. *G* – photograph of a fragment from 60 μm-thick section immunolabeled with NeuN for mature neurons. In the reconstructions *Ax* and *Den* stand for an axon and dendrite correspondingly; arrow in the ON shows rostro-caudal direction. Scale bars are equal to 100 μm in all drawings and on the photo.

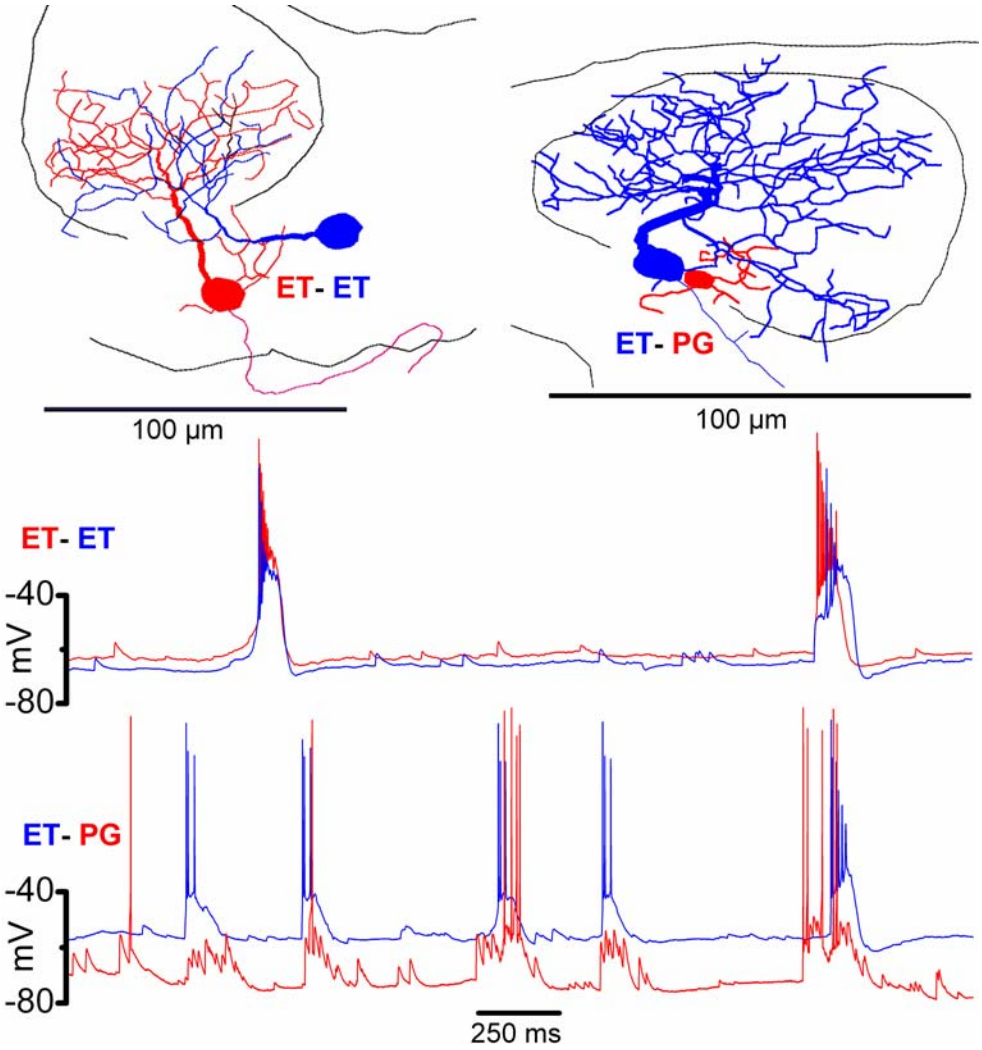

Figure 3. Synchronous activity among JG cells associated with the same glomerulus. Upper panel shows reconstructions of the recorded cells (left, 2 ET cells; right, an ET and a PG cells). Middle panel: Dual whole-cell current clamp recording from two ET cells (red and blue traces, respectively) showing correlation of spike bursts and membrane potentials. Lower panel: Dual whole-cell current clamp recordings show that EPSP-bursts and spikes in the PG cell (red trace) are synchronous with spike-bursts in the ET cell (blue trace).

ET cells. These are the largest (10-15 µm) cells in the GL, and electrophysiological recordings have confirmed that they are excitatory. Their cell bodies are situated in the deep half of the glomerular layer. Most have one apical dendrite that arborizes extensively throughout one glomerulus (Fig.2*B*) [Pinching and Powell, 1971a; Hayar et al., 2004a,b]. Rarely, ET cells have 2 or 3 apical dendrites that ramify in different glomeruli. In earlier studies most ET cells were shown to have secondary dendrites that extend in the superficial EPL [Macrides and Schneider, 1982]; however, in slices only one third of ET cells were found to possess secondary dendrites [Antal et al., 2006]. ET cells are the output neurons for the GL, because their axons project into deeper layers of the MOB. Axons of ET cells vary in their patterns and possible targets; some axons emit short collaterals in the GL and EPL before entering internal plexiform and granule cell layers, whereas axons of other ET cells cross through EPL with little branching [Antal et al., 2006]. Axons of some ET cells situated

in the lower third of the GL create intrabulbar associational system providing point-to-point reciprocal projections between opposing regions of the medial and lateral MOB [Schoenfield et al., 1985; Liu and Shipley, 1994]. Presence of processes descending from GL into EPL is a decisive anatomical criterion that distinguishes ET from PG cells, because PG cells are local neurons of the GL and their axons and secondary dendrites, when present, do not leave the GL (Pinching and Powell, 1971a).

The most distinctive physiological feature of ET cells is their spontaneous rhythmical bursting, where bursting is defined as generation of spike clusters regardless of their interspike intervals within bursts (Figure 3) [Hayar et al., 2004a]. Glomerular layer cells with burst characteristics have been reported *in vivo* [Getchell and Shepherd, 1975; Wellis and Scott, 1990]. The rhythmical burst-firing mode was characteristic of morphologically confirmed ET neurons [Hayar et al., 2004a]. By contrast, PG and SA cells do not spontaneously generate spike bursts nor can they be induced to burst by intracellular current injections. ET cell burst frequencies range from ~1 to 8 Hz, with a mean of 3.3 ± 0.18 bursts/s. This range overlaps with the delta-theta frequency range (1-10 Hz) prominent in oscillatory neural activity in the rodent olfactory network. The delta range includes components related to low frequency (1-3 Hz) "passive" sniffing, whereas a higher frequency theta-component (5-10 Hz) is characteristic for "active" investigative sniffing [Adrian, 1950; Welker, 1964; Macrides et al., 1982; Eeckman and Freeman, 1990; Kay and Laurent, 1999; Kay, 2003]. ET cells also receive spontaneous bursts of IPSCs from PG cells [Hayar et al., 2004b]. ON stimulation evokes an EPSC in ET cells that is followed by IPSC bursts [Hayar et al., 2004b]. Both the spontaneous and ON-evoked IPSCs in ET cells are driven primarily by activation of AMPA receptors.

Several lines of evidence indicate that bursting is an intrinsic property of ET cells. First, bursting deteriorates rapidly after establishment of whole-cell recording mode. This pronounced "rundown" of bursting may explain the low reported incidence of spontaneous bursting in JG cells in some whole-cell recording studies [Bardoni et al., 1995; Puopolo and Belluzzi 1996, 1998; McQuiston and Katz, 2001]. The rundown of bursting could be due to intracellular dialysis of an intracellular messenger important to maintain spontaneous activity [Alreja and Aghajanian, 1995]. Additional evidence in support of the intrinsic mechanism for bursting are the findings that: (1) burst frequency is voltage-dependent and (2) bursting persists in blockers of ionotropic and metabotropic glutamate receptors, and $GABA_A$ receptors. Moreover, spontaneous bursting was not blocked by Cd^{2+}, which suppresses Ca^{2+}-dependent neurotransmitter release, ruling out the potential involvement of other neurotransmitters. Depolarizing current injections evoke in ET cells low-threshold Ca^{2+} spikes (LTS) that were eliminated by the calcium channel blockers, Cd^{2+} (100 μM) and Ni^{2+} (1 mM) [McQuiston and Katz, 2001; Hayar et al., 2004a]. This suggested that the LTS is one of mechanisms for burst generation in ET cells. However, there is a line of evidence for another mechanism for generation of spike clusters. First, bursting (or rather grouping spikes in clusters with randomly varying inter-spike intervals (ISI) within groups) persisted after the LTS was blocked. Second, ET cell bursting was abolished by extracellular TTX or by intracellular QX-314, whereas the LTS persisted. Moreover, low concentration of the sodium channel blocker (TTX, 10 nM, which is known to block the persistent sodium current without significantly affecting the fast sodium spikes [Azouz et al., 1996; Brumberg et al., 2000; Su et al., 2001]) progressively decreased the number of spikes in the burst and eventually transformed bursting into single spike firing. The bursting recovered after washout of TTX (Figure 4).

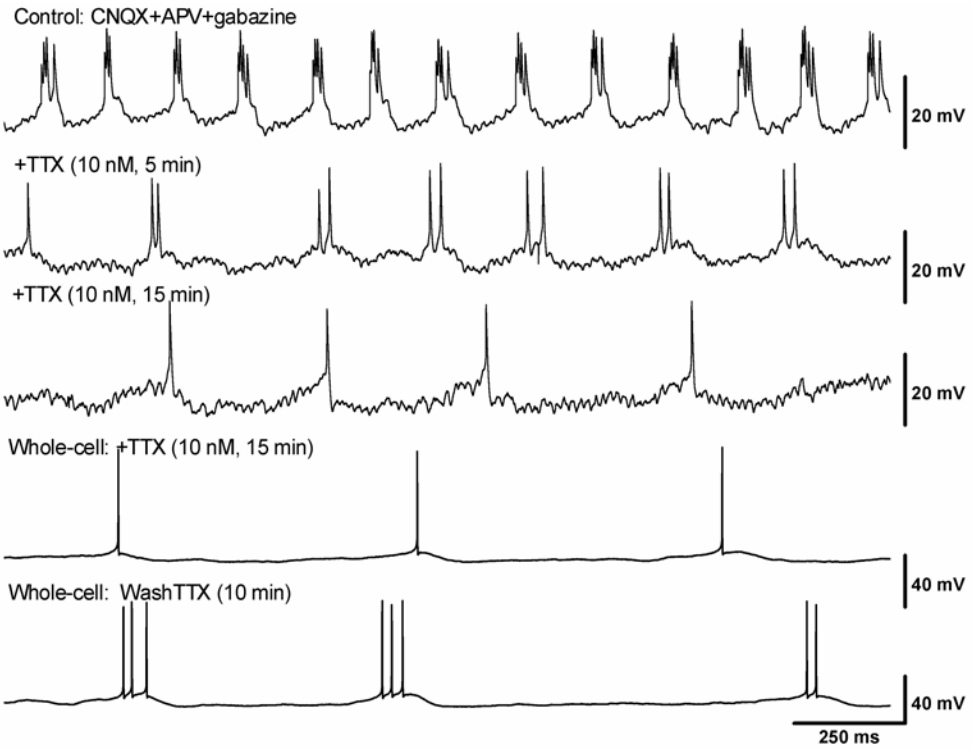

Figure 4. Sodium channels are essential for spontaneous burst generation. A bursting ET cell was recorded in the presence of synaptic blockers in cell-attached mode to prevent bursting rundown due to intracellular dialysis in whole-cell mode. A low concentration of the sodium channel blocker (TTX 10 nM) progressively decreased the number of spikes in the burst and eventually transformed bursting into single spike firing as also seen when recording was switched to whole-cell mode. The bursting recovered after washout of TTX.

Third, the activation threshold of the LTS (-38 mV) was approximately 15 mV more depolarized than the membrane potentials from which bursting arises, on average –53 mV. Calcium may modulate bursting as calcium channel blockers prolonged burst duration [Hayar et al., 2004a]. Calcium channel blockers also increased the inter-burst interval but this could be due to a charge screening effect. Moreover, ET cells have a hyperpolarization-activated cation conductance (I_h) that is prominent at resting membrane potentials (unpublished observations). I_h participates in burst timing and rhythmicity [DiFrancesco 1993; Lüthi and McCormick 1998; Pape 1996] and is modulated by calcium. Thus, I_h and calcium may play a role in burst termination and/or setting the inter-burst interval.

Rhythmic membrane potential oscillations (MPOs), but not the LTS, were blocked by extracellular TTX and by intracellular dialysis with QX-314. These results suggest that, as for many cortical and hippocampal neurons [Azouz et al., 1996; Brumberg et al., 2000; Su et al., 2001], burst generation in ET cells requires slowly inactivating Na^+ channels, i.e., a persistent sodium current. Indeed, all ET cells tested had a prominent TTX-sensitive, persistent inward current. The characteristics of this current are well suited to trigger spontaneous bursting in ET cells. The inward current activates near -60 mV, slightly hyperpolarized to the mean ET cell resting potential (-52 mV). Thus, it is reasonable to conjecture that as this persistent sodium current slowly depolarizes the ET cell membrane, additional sodium channels are activated further depolarizing the membrane to the threshold for action potential generation. This current maintains a level of depolarization sufficient to generate additional action potentials until another mechanism(s), possibly involving calcium (see above), terminates the

burst by transiently hyperpolarizing the membrane below the activation threshold for the persistent sodium current. As the membrane re-polarizes, the persistent sodium current is re-engaged and the burst cycle is repeated. We conclude that persistent sodium channels are essential and required for the generation of spontaneous bursting [Hayar et al. 2004a]. Calcium channels may play a modulatory role especially in bursts evoked by depolarizing currents or following negative current injections [McQuiston and Katz, 2001; Zhou et al., 2006].

The relative contribution of persistent sodium current, I_h current, and low threshold calcium current may account for possible differences in bursting patterns of glomerular tufted cells. The majority of ET neurons generate classical bursts of 3-6 spikes with slightly incremental inter-spike intervals (ISIs) followed by a slow afterhyperpolarization (sAHP) [McQuiston and Katz, 2001; Hayar et al., 2004a; Zhou et al., 2006]. The remaining ET cells generate groups of spikes with unequal and irregular interspike intervals within groups and without following sAHP. After we divided a set of recorded ET cells in two subsets, 27 of them demonstrated one or more classical bursts upon current injection and 22 have shown either strong accommodation or grouping of spikes on a current step. Spontaneous activity of the first group was characterized by bursts with pronounced depolarization envelopes, whereas spontaneous activity of the second group contained spike clusters with various ISIs riding on slow waves of membrane potential (V_m). We noticed, that ET cells with short (<50 μm) shaft of a primary dendrite (short-shafted cells, SS-ET) often generated classical bursts in spontaneous activity and on a current step, whereas ET cells with longer (>50 μm) primary dendrite (long-shafted, LS-ET) often had secondary dendrites ramifying in the EPL and typically fired groups or irregular spikes (Table 1). Correspondence between physiological and anatomical features in our experiments was not significant, although we employed additional parameters such as V_m, input resistance (R_{in}), magnitude of fast afterhyperpolarization after a spike (fAHP) and coefficient of spike accommodation upon current injection (AccC = accommodation coefficient = ratio of the first and the last ISI; current injection = 500 ms) (Table 2). Nevertheless, recently a very thorough statistical analysis of ET cell physiology and anatomy has proven that indeed, there are two subtypes of ET cells [Antal et al., 2006]. Employing principal component analysis and agglomerative clustering analysis, the authors have shown that a set of electrophysiological (e.g. burst firing on a depolarizing current step) and morphological (e.g. lack of basal dendrites) parameters of ET cells are highly predictive of one another. Twenty four of thirty measured parameters, including length of a primary dendritic shaft, significantly differed between the two ET subpopulations. Qualitatively the most prominent difference was that the absence of basal dendrites correlated with spike bursting (65% of cells) and vice versa, the presence of basal dendrites correlated with the lack of spike bursting (35%).

Table 1. Firing pattern on a depolarizing current pulse

Cell type	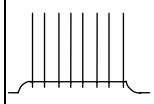 Regular firing AccC>0.7	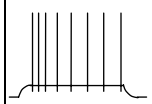 Weak Accommodation 0.3>AccC>0.7	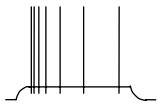 Strong Accommodation AccC<0.3	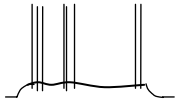 Grouping, no sAHP after burst	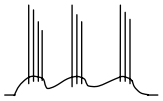 Repetitive bursts, sAHP after burst	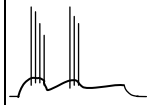 Adapting bursts, sAHP after burst	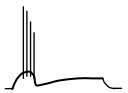 One initial burst	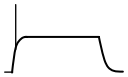 1 or 2 initial spikes followed by plateau-potential	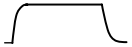 No spikes, plateau-potential
SA (n=11, 8.3%)	•••• ••• 7	•••• 4							
PG (n=39, 29.5 %)	••••• •••• •••• 13	••••• •••••• •••••• 17	•• 2				• 1	••••• •••••• •••••• •••••• •••• 27	•• •••• 6
LS-ET (n=15, 11.3%)	•• 2	••• 3	••• 3	••• 3	••• 3	• 1			
SS-ET (n=40, 30.3 %)		• 1	••••• ••••• ••• 13	••• 3	•• •••• 6	••••• •••• 9	•••• •••• 8		

Total amount of JG cells recorded N = 132.

Table 2. Functional parameters of JG cells (M ± SE)

Parameter	SA N=11	CPG N=23	HPG N=17	LSET N=13	SSET N=25
V_m (mV)	-62.3 ± 1.3	-63.8 ± 1.8	-59.9 ± 2.9	-60.9 ± 1.6	-58.3 ± 1.9
R_{in} (MΩ)	642 ± 114	866 ± 114	1458 ± 185	512 ± 160	370 ± 48
τ (ms)	21.6 ± 4.1	25 ± 2.4	19.4 ± 3.7	21.2 ± 4.1	18.8 ± 3.2
AP threshold (mV)	-34.4 ± 2.1	-36.1± 1.6	-38.2 ± 1.5	-43.1 ± 0.8	-30.5 ± 4.8
AP half-width (ms)	0.81 ± 0.09	0.88 ± 0.06	0.87 ± 0.10	0.66 ± 0.05	0.77 ± 0.08
AP asymmetry	2.24 ± 0.11	2.45 ± 0.20	2.15 ± 0.19	2.42 ±0.17	2.4 ± 0.19
fAHP (mV)	-20.8 ± 1.3	-14.7 ± 1.5	-4.8 ± 1.9	-5.8 ± 1.6	-6.8 ± 1.3
AccC	0.8 ± 0.06	0.55 ± 0.06	0.77 ± 0.04	0.44 ± 0.12	0.15 ± 0.02
Response latency upon ONL stimulation (ms)	2.5 ± 0.3	3.1 ± 0.5	4.6 ± 0.5	2.9 ± 0.9	2.2 ± 0.2

* *AP threshold* – threshold for initiation of action potential. *AP half-width* – duration of the action potential at half of its amplitude. *AP asymmetry* – ratio of decay duration to rise duration in a single spike or the first spike of a burst. *fAHP* – fast afterhyperpolarization after a spike. *AccC* – accommodation coefficient: ratio of the first and the last interspike intervals in firing patterns upon injection of depolarizing current.

Besides, ET cells with basal dendrites possessed a much larger and more extensively ramifying axonal arbor. This one third of the ET population can receive sensory input not only from their own glomerulus, but from other modules in the GL and from granule cells in the EPL. Through rich axonal ramifications these ET cells can coordinate broad area in the EPL (~400 μm diameter, unpublished observation), thus creating the second order module (module of the first order is the glomerulus-associated neuronal ensemble). In turn, bursting ET cells without secondary dendrites mostly communicate with neurons in their own glomerulus. This subtype of ET cells demonstrated the highest degree of spontaneous burst synchrony in our experiments [Hayar et al., 2004b]. On the other hand, it is possible to consider those ET cells that have long primary shafts and secondary dendrites as displaced EPL tufted cells because their properties are similar to superficial tufted cells (unpublished observations).

PG cells. These cells are the most numerous cells in the GL, and they are thought to be inhibitory in nature. They have small (5-8 μm), spherical or ovoid somata, and they are distributed in the periglomerular regions surrounding the glomeruli. Their dendrites are typically restricted to a small subregion of a glomerulus [Pinching and Powell, 1971a; Hayar et al., 2004a,b] and receive asymmetrical (morphologically excitatory) synapses from ET and mitral/tufted cells dendrites. We found that not all of biocytin filled PG cells had dendritic tree of a classical shape with one or two robust primary dendrites described by Pinching and Powell [1971a]. A portion of PG cells had only one to four extremely fine poorly branching short hair-like dendrites, which almost did not taper from the base to the tips. Therefore we named these cells hairy periglomerular (HPG) cells (Fig.2*C*) to distinguish them from classical periglomerular (CPG) cells (Fig.2*A*). Since HPG and CPG cells had overlapping functional parameters (Table 2), we presume that HPG represent immature PG cells developing from progenitor cells, which continuously migrate to the GL from subventricular zone [Baker and Margolis, 2002; Coskun and Luskin, 2002; Fukushima et al., 2002]. This

hypothesis is confirmed by the fact that some HPG cells in response to current injection produced only a plateau-potential, but did not generate fast spikes (last column in Table 1) – the behavior characteristic to progenitor cells [Storch et al., 2003; Wang et al., 2003; Westerlund et al., 2003]. Despite the observed diversity in morphology among PG cells, we still consider them as a single type of JG neurons.

Physiological recordings indicate that PG cells receive monosynaptic dendrodendritic excitatory input from ET cells and only a relatively small subpopulation of PG cells receives direct input from ON terminals [Hayar et al., 2004b]. Some of the mitral/tufted-to-PG cell synapses are paired with reciprocal symmetrical (morphologically inhibitory) synapses (usually from other PG cells) back onto the parent mitral/tufted cell dendrites [Pinching and Powell, 1971b; Kasowski et al., 1999; Toida et al., 1998, 2000]. The axons of PG cells are rare, but have been reported to extend over distances equivalent to 4-5 glomeruli [Blanes, 1898; Pinching and Powell, 1971a; Hayar et al., 2004a]. They appear to form symmetrical (morphologically inhibitory) synapses onto mitral/tufted cell dendrites and onto ET cells and other JG cells [Pinching and Powell, 1971c]. Most PG cells are GABAergic [Ribak et al., 1977; Mugnaini et al., 1984; Kosaka et al., 1985, 1987a,b,c,d, 1988]. The GL also contains the largest population of dopamine (DA)-containing cells in the brain. The majority of dopaminergic cells are PG cells, but some ET cells are also dopaminergic [Halász et al., 1977; Davis and Macrides, 1983; Halász et al., 1985; Gall et al., 1986; McLean and Shipley, 1988]. Therefore, the dopaminergic PG neurons are regarded as a subpopulation of GABAergic neurons.

An estimated, 10% of PG neurons in adulthood are positive for tyrosine hydroxylase (TH) [McLean and Shipley, 1988; Kratskin and Belluzzi, 2003], the rate-limiting enzyme for dopamine synthesis. Dopaminergic neurons have been recently identified *in vitro* using a transgenic mouse strain harboring an eGFP (enhanced green fluorescent protein) reporter construct under the promoter of tyrosine hydroxylase. The most prominent feature of these cells when recorded in acutely dissociated cell culture preparations was the presence of regular spontaneous spiking at ~8 Hz. In these cells, five main voltage-dependent conductances were identified [Pignatelli et al., 2005]: a fast transient Na^+ current, a delayed rectifier K^+ current, a persistent Na^+ current, and LVA and HVA Ca^{2+} currents. The MPOs are supported by the interplay of the persistent Na^+ current and of a T-type Ca^{2+} current.

The spontaneous activity patterns of PG cells in slices differ markedly from ET cells. PG cells have relatively low levels of spontaneous spike activity and lack the capacity to generate voltage-dependent MPOs and spike bursts in response to depolarizing currents [Hayar et al., 2004a,b]. In slices, spikes in PG cells are driven primarily by spontaneous glutamatergic EPSPs. However, because of their heterogeneous neurochemical characteristics, PG cells are also likely to be functionally heterogeneous. For example, some studies have reported that different PG cells subtypes appear to exhibit different K^+ conductances [Puopolo and Belluzzi 1998] as well as different firing behaviors [McQuiston and Katz 2001]. In agreement with this, we found that anatomically identified PG cells had two basic firing patterns. In response to injection of depolarizing current they either fired regular/weakly accommodating spikes, or produced one or two initial spikes followed by a plateau-potential (Table 1).

SA cells. These cells are roughly the same size (8-12 μm) as ET cells. They are distinguished by only a few poorly branching dendrites, which are not associated with any particular glomerulus, but extend for 200-300 μm in arbitrary directions (Fig.11*E*). Therefore, they seem to harvest information from inside of multiple glomeruli and interglomerular space

[Aungst et al, 2000; Hayar et al., 2004b]. They are thought not to receive direct ON input [Pinching and Powell, 1971c; Hayar et al., 2004b]. The dendrites of SA cells may receive excitatory synaptic inputs from ET cells [Hayar et al., 2004b], tufted and mitral cell dendrites or from other SA cells. Inhibitory synaptic inputs on SA cells from PG cells have not been shown. SA cells have axons that can extend up 1-2 mm within the GL [Aungst et al., 2003]. The axons were thought to synapse onto the dendrites of PG cells [Pinching and Powell, 1971a], but they seem to synapse also on ET cells [Aungst et al., 2003]. The resting spontaneous activity patterns of SA cells slices appears to be very similar to that of PG cells with characteristic bursts of EPSP/Cs [Hayar et al., 2004b]. Upon injection of a depolarizing current SA cells fire regular spikes with a weak or no accommodation (AccC > 0.7, Table 1). The functional significance of SA cells will be discussed later.

According to the morpho-physiological data obtained so far on JG cells, we suggest a set of criteria to facilitate targeting of a desired JG cell type in neurophysiological experiments in slices. Despite partial overlap of electrophysiological parameters, their combination with high probability helps to identify a neuron. We consider three qualitative and three quantitative properties of a cell: a) morphology, b) firing pattern upon current injection, c) response to ON stimulation and spontaneous activity, d) R_{in}, e) fAHP, f) AccC. Now we can describe the most probable features of each anatomically defined cell type.

1) A neuron is an ET cell if *(i)* its dendritic tuft ramifies in most of the glomerulus and its processes (axon and/or secondary dendrites) descend in EPL, *(ii)* it demonstrates voltage-dependent intrinsic membrane potential oscillations and bursts or groups of spikes. Physiological parameters should be: R_{in} < 500 MΩ, AccC < 0.3 (for SS-ET), 0 < fAHP < 15 mV, the latency of EPSP/C upon ONL stimulation is constant with a jitter<0.5 ms.
2) A neuron is a SA cell if it has arbitrarily oriented poorly branching dendrites and long axonal processes exclusively within the GL. Besides, it must show *(i)* regular or weakly adapting firing on a current step, *(ii)* spontaneous and evoked EPSP/C bursts, *(iii)* deep fAHP (> 10 mV).
3) A neuron is a HPG cell if it has fine hair-like short and poorly branching processes mostly directed into the glomerular neuropil. Most probably, it can generate spontaneous or current injection-driven plateau-potentials. It does not generate fast spikes at all, or fires only one initial spike followed by a plateau-potential. Spontaneous and evoked EPSP/C bursts are well pronounced, fAHP after a single initial spike is small (< 10 mV) and R_{in} is high (~ 1GΩ and more).
4) Periglomerular cells of a classic shape are characterized by odd dendritic morphology. They have one or more primary dendritic shafts in one glomerulus, all without distinctive tufts and no or very short axon, sometimes invading an adjacent glomerulus. Basically, CPG cells have high R_{in} (> 400 MΩ), deep fAHP (> 13 mV), weak or no accommodation, spontaneous and evoked EPSP/C bursts. However, some neurons with the CPG anatomy possessed HPG-like membrane properties, apparently indicating a transition between HPG and CPG. In contrast to our data other authors have shown Ca^{2+}-dependent plateau-potentials not only in PG, but also in ET cells [Zhou et al., 2006]. These plateau potentials described by Zhou et al. (2006) resemble the previously described LTS in ET cells [McQuiston and Katz, 2001;

Hayar et al., 2004a] but had longer duration because recordings were mostly performed at room temperature.

5. ON GLUTAMATERGIC SYNAPTIC INPUT TO JG CELLS

Glutamate is the major transmitter released by ON axons onto the dendrites of JG neurons, as well as those of mitral/tufted cells in the GL. Release of glutamate from ON terminals is controlled by N- and P/Q-type Ca^{2+} channels [Isaacson and Strowbridge, 1998]. Each glomerulus contains the apical dendritic tufts of about 20 mitral cells, 200 tufted cells and 1500 - 2000 JG cells [reviewed in Shipley et al., 1996]. A variety of studies demonstrated that sensory transmission from ON axon terminals is mediated by glutamate acting primarily at AMPA and NMDA ionotropic glutamate receptor subtypes [Bardoni et al., 1996; Ennis et al., 1996, 2001; Aroniadou-Anderjaska et al., 1997; Chen and Shepherd, 1997; Keller et al., 1998]. Comparatively less is known about the role of mGluRs at ON synapses, although metabotropic glutamate receptors (mGluRs) are expressed by nearly all MOB neurons [Ennis et al., 2006]. Electrophysiological and Ca^{2+}-imaging studies have reported that ON stimulation evokes an mGluR1-sensitive synaptic component in ~40% of mitral cells in normal physiological conditions in the slice [De Saint Jan and Westbrook; 2005; Ennis et al., 2006; Yuan and Knopfel, 2006]. mGluR1-mediated responses were maximal with bursts of 50-100 Hz ON spikes, similar to frequencies of odor-induced spikes in ORNs *in vivo* [Duchamp-Viret et al., 1999]. Activation of mGluRs has also been suggested to produce long-term depression at ON-to-mitral cell synapses [Mutoh and Knopfel, 2005].

All ET cells receive monosynaptic ON input, which appears to be primarily mediated by AMPA receptors in normal physiological conditions *in vitro* [Hayar et al., 2004a,b]. If the amplitude of an ON-evoked EPSP reaches threshold for spike generation, a spike burst is always triggered in ET cells [Hayar et al, 2004a]. Further increases in ON stimulation strength produce the same all-or-none burst. Thus, ET cells receive monosynaptic ON input that is converted into an all-or-none spike burst. Accordingly, ET cells amplify suprathreshold sensory input at the first stage of synaptic transfer in the olfactory system. ET cells also readily entrain to rhythmic ON input delivered at theta frequencies (5-10 Hz) characteristic of investigative sniffing in rodents [Hayar et al., 2004a].

The majority of PG cells exhibit longer latency, prolonged bursts of EPSP/Cs in response to ON stimulation than ET cells. The long, variable latency of these responses is indicative of di- or polysynaptic ON input. Thus, most SA and PG cells do not appear to receive direct ON input, perhaps because their dendrites ramify in glomerular compartments devoid of ON terminals. Only 20% of PG cells had short, relatively constant latency EPSCs following ON stimulation and in some of these cells the short latency synaptic response was followed by a delayed burst of EPSP/Cs. SA cells also responded to ON stimulation with long, variable latency, prolonged bursts of EPSP/Cs and never exhibited responses consistent with monosynaptic ON input. These findings indicate that (1) SA cells and most PG cells lack direct ON input and (2) ET cells along with mitral/tufted cells are the major postsynaptic targets of ON inputs.

Since most (~80%) PG cells, and all SA cells, lack monosynaptic ON input, this suggests that most PG cells are functionally associated with glomerular compartments lacking ON

terminals. Anatomical studies have revealed that the glomeruli have a bi-compartmental organization. Each glomerulus has two types of intermingled compartments, one of which is rich in ON terminals and the second of which is devoid of ON input [Kosaka et al., 1997; Kasowski et al., 1999]. Calbindin-positive JG neurons extend their dendrites only into glomerular compartments devoid of ON terminals, suggesting that they do not receive direct sensory innervation [Toida et al., 1998; 2000]. It is reasonable to speculate, therefore, that the SA and PG cells that do not receive direct input [Hayar et al., 2004b] may correspond to these calbindin-positive JG neurons.

These PG cells might provide localized inhibition to mitral/tufted cell dendrites, or to nearby dendrites of other JG cells. Dopaminergic and GABAergic PG cells presynaptically inhibit ON terminals [Hsia et al., 1999; Wachowiak and Cohen, 1999; Aroniadou-Anderjaska et al., 2000; Berkowicz and Trombley, 2000; Ennis et al., 2001; Murphy et al., 2005; Wachowiak et al., 2005]. Since at least 20% of PG cells receive monosynaptic ON input, it is possible that these cells primarily mediate this presynaptic inhibition of the ON. In contrast to PG cells, SA cells extend dendrites and axons across multiple glomeruli, and are thought to be involved in inter-glomerular communications [Aungst et al., 2003].

6. SPILLOVER OF DENDRITICALLY RELEASED GLUTAMATE

As noted above, the apical dendrites of ET and mitral/tufted cells that ramify in the glomeruli are glutamatergic. Although the dendrites of these cell types do not form synapses with each other, the release of glutamate from the apical dendrites has been reported to produce non-synaptically-mediated excitation (i.e., glutamate spillover) of the parent cell releasing glutamate (self- or auto-excitation) or neighboring cells. Such excitation is facilitated by removal of Mg^{2+} from the extracellular media, which enhances activation of NMDA receptors. Alternatively, spillover-mediated excitatory responses can be facilitated in the presence of physiological levels of extracellular Mg^{2+} by blockade of $GABA_A$ receptors [Salin et al., 2001; Freidman and Strowbridge, 2000]. Under such conditions, intracellular depolarization of individual mitral cells produces long duration, NMDA-receptor-dependent excitation of the same cell or adjacent mitral cells [Aroniadou-Anderjaska et al., 1999; Isaacson, 1999; Salin et al., 2001; Freidman and Strowbridge, 2000; Christie and Westbrook, 2006]. ET cells have also been reported to exhibit such self-excitation [Murphy et al., 2005]. The mitral cell self-excitation can be blocked by intracellular Ca^{2+} chelation or blockade of voltage-gated Ca^{2+} channels [Salin et al., 2001; Freidman and Strowbridge, 2000]. The self-excitation responses are graded and increase with the number of spikes or depolarizing pulses applied to the mitral cell [Salin et al., 2001; Freidman and Strowbridge, 2000]. It has been suggested that the NMDA autoreceptors may serve to increase the firing frequency of mitral cells during prolonged discharges [Friedman and Strowbridge, 2000]. Such excitation can also be evoked by antidromic activation of mitral cells [Chen and Shepherd, 1997; Aroniadou-Anderjaska et al., 1999]. This glutamate spillover mediated, NMDA receptor-dependent excitation appears to occur chiefly among the lateral dendrites of mitral cells, while an AMPA receptor-dependent spillover occurs among the apical dendrites of mitral/tufted cells [Aroniadou-Anderjaska et al., 1999; Salin et al., 2001; Schoppa and Westbrook, 2001, 2002; Christie and Westbrook, 2006]. Electrotonic coupling among mitral

cell dendrites in the same glomerulus facilitates spillover responses mediated by AMPA receptors [Schoppa and Westbrook, 2002; Christie and Westbrook, 2006].

Other glomerulus-specific glutamate-mediated excitatory interactions among mitral cells have been reported. Reciprocal glutamate-mediated excitation was reported between closely adjacent mitral cells, whose apical dendrites extended into the same glomerulus [Urban and Sakmann, 2001]. The latency for the mitral-to-mitral cell EPSPs was surprisingly short, in-line with monosynaptic mediation, despite the fact that mitral cells do not form anatomical synapses with each other. The EPSP was primarily mediated by AMPA receptors and originated within the glomerular layer, suggesting that they are generated in the apical dendrites of mitral cells. In contrast to the preceding studies, Carlson et al. [2000] reported that ON stimulation, antidromic activation of multiple mitral/tufted cells, but never activation of single mitral cells, elicited long-lasting depolarizations (LLDs) in mitral cells. The LLDs were all-or-none in nature, required activation of AMPA receptors, and originated in the glomeruli. Further, spontaneous LLDs were synchronous among mitral cells associated with the same, but not different glomeruli. The LLDs appear to be a network phenomenon, presumably reflecting recurrent, intraglomerular glutamate release from dendritic tufts of a mitral/tufted cell ensemble.

7. ET CELL DENDRODENDRITIC INPUT TO PG AND SA CELLS

As noted above, ET and mitral/tufted cells form excitatory glutamatergic dendrodendritic synapses with PG and SA cells in the glomeruli. PG cells, and perhaps SA cells, in turn form inhibitory GABAergic dendrodendritic synapses with ET and mitral/tufted cells. Compared to the dendrodendritic synapses between mitral/tufted and GCs in the EPL, far less is known about the properties of the dendrodendritic synapses in the GL. PG and SA cells were reported to receive spontaneous bursts of glutamatergic EPSCs [Hayar et al., 2004b]. Since SA cells and most PG cells do not receive direct ON input, this input must arise from other excitatory elements within the glomeruli. Prime candidates include the apical dendrites of ET cells and mitral tufted cells. Spontaneous spike bursts or direct depolarization of individual ET cells to elicit spike bursts was reported to trigger EPSC bursts in PG and SA cells mediated by activation of AMPA receptors [Hayar et al., 2004b]. The latency of the evoked EPSCs (0.85 ms) was indicative of monosynaptic input to PG cells from ET cells. Additional studies demonstrated that this ET cell to PG cell excitatory transmission is intraglomerular as it was only observed between cells associated with the same glomerulus. Stimulation of an individual ET cell was reported to produce large EPSCs and Ca^{2+} spikes in PG cells [Murphy et al., 2005]. The NMDA receptor antagonist APV had minimal effects on the EPSP but abolished the Ca^{2+} spike. The same study reported that stimulation of single ET cell excites 2-7 unidentified JG cells within the same glomerulus, suggesting that individual ET cells synapse with multiple PG cells.

Single spikes in PG cells are relatively ineffective in triggering GABA release from PG cells [Murphy et al., 2005]. Multiple spikes, leading to low-voltage activated (LVA) Ca^{2+} currents, are much more effective in releasing GABA from PG cells [Murphy et al., 2005]. These findings suggest that GABA release from PG cells may be preferentially triggered when these cells receive strong synaptic input. ET cells, individually and collectively, provide

strong input to PG cells. Spike bursts in individual ET cells robustly activate PG cells. Additional, individual ET cells appear to activate, on average, 5 PG cells [Murphy et al., 2005]. There is now growing evidence suggesting that the spiking and synaptic activity of ET, tufted and mitral cells are correlated due to the presence of electrical synapses and glutamate spillover among cells of the same type and possibly cells of different types (unpublished observations by Abdallah Hayar). The dendrodendritic interactions between these cells and PG cells ensure a synchronous excitatory bursting input to PG cells leading to the generation of few spikes or a spike followed by plateau potential leading to calcium influx into PG cell dendrites and the release of GABA onto ET, tufted and mitral cells.

PG cells contain GABA and thus activation of these cells will cause dendrodendritic inhibition of ET and mitral/tufted cell dendrites in the glomeruli. In the periglomerular spaces, their axons also form symmetrical synapses onto the mitral/tufted cell dendrites and onto PG and SA cells [Pinching and Powell, 1971c]. Physiological studies support the notion that PG cells receive excitatory input from mitral/tufted cells and ET cells, and in return, make feedforward and feedback inhibitory GABAergic synapses onto these cells [Shepherd and Greer, 1998; Hayar et al., 2004b]. Such inhibition is thought to be primarily mediated by $GABA_A$ receptors. Intracellular depolarization of ET cells leads to GABAergic inhibition due to activation of dendrodendritic synapses with PG cells [Murphy et al., 2005]. Using this paradigm, the feedback inhibition produced by ET cell depolarization was reduced by nimodopine, a blocker of L-type Ca^{2+} channels; nimodipine, however, did not reduce GABA release from PG cells. Subsequent experiments, using paired recordings of PG cells, suggested that GABA exocytosis from these cells is governed primarily by activation of high-voltage-activated (HVA), P/Q-type Ca^{2+} channels. The L-type antagonist nimodipine did not alter GABA release from PG cells, leading to the conclusion that activation of LVA currents can facilitate GABA release from PG cells, but these channels are not directly coupled to GABA exocytosis. These studies and others [Smith and Jahr, 2002] also indicate that PG cells, under certain circumstances, can release GABA onto themselves, and perhaps neighboring PG cells. GABA has been reported to depolarize PG cells at their resting potential, probably due to elevated intracellular chloride concentrations [Siklos et al., 1995; Smith and Jahr, 2002]. It was suggested that GABA inhibits PG cells by activating a chloride conductance that reduces the neuronal input resistance and shunts excitatory inputs. GABA released from PG cells was recently shown to inhibit other PG cells in the same glomerulus via GABAA receptors [Murphy et al., 2005]. Because PG cell dendrites ramify within a restricted portion of a glomerulus, their functional interactions are presumably localized to microdomains of the extensive mitral/tufted cell dendritic arbors, or to nearby JG cells [Kasowski et al., 1999].

8. PRESYNAPTIC INHIBITION OF ON TERMINALS

DA and D2 receptors. The rat MOB contains more DA neurons (100,000-150,000; McLean and Shipley, 1988) than the entire substantial nigra and ventral tegmental area midbrain DA system (~30,000) [Björklund and Lindvall, 1984]. But the MOB receives no known extrinsic DA input. The ONL and GL have high densities of D2 receptors in rats and mice [Coronas et al., 1997; Koster et al., 1999; Levey et al., 1993; Mansour et al., 1990;

Nickell et al., 1991]. In the GL, the JG neurons express D2 receptors (Mansour et al., 1990). Other anatomical evidence indicates that most, if not all, of the D2 receptors in the GL occur on ON axon terminals. ORNs express D2 receptors and bulbectomy, a manipulation that causes retrograde degeneration of ORNs, eliminates D2 receptor mRNA in the olfactory epithelium [Koster et al., 1999]. Taken together, these findings indicate that DA released from JG neurons may presynaptically modulate ON terminals via activation of D2 receptors.

In agreement with this, DA and D2 receptor agonists reduced spontaneous and ON-evoked activity in mitral cells, as well as odor-evoked activity in the GL and odor detection performance, in a variety of species [Nowycky et al., 1983; Doty et al., 1989; Sallaz and Jourdan, 1992; Hsia et al., 1999; Wachowiak and Cohen, 1999; Berkowicz and Trombley, 2000; Ennis et al., 2001]. These effects are mediated by presynaptic suppression of glutamate release from ON terminals via inhibition of Ca^{2+} influx [Wachowiak and Cohen, 1999]. In a similar manner, DA and D2 receptor agonists suppressed spontaneous and ON-evoked activity in JG cells, but had no effect on mitral to JG cell transmission [Ennis et al., 2001]. The inhibitory effects of DA were abolished in D2 receptor knockout mice [Ennis et al., 2001]. Presynaptic inhibition of ON terminals by DA provides a mechanism for increasing the range of concentrations that can be processed by MOB neurons: as activity increases in ON terminals, DA JG cells are more strongly excited. This, in turn, provides negative feedback onto ON terminals reducing the release of glutamate. Such a scheme would effectively increase the dynamic range of information transfer from ORNs to MOB neurons. Interestingly, systemic administration of D2 receptor agonists has been reported to prevent odorant specific 2-deoxyglucose patterns in MOB and to reduce odorant detectability [Doty and Risser, 1989; Sallaz and Jourdan, 1992]. Related to this question of how DA participates in odor processing is the degree to which these receptors are tonically active *in vivo*? If, for example, ON terminals are tonically inhibited by DA via D2 receptors, this might serve to filter out weak signals ("noise"). This might sharpen the spatial pattern of active glomeruli, and facilitate detection of predominant odors. There is experimental support for this possibility. Blockade of D2-like receptors by systemic administration of spiperone increased the number of mitral cells that responded to single or multiple odorants [Wilson and Sullivan, 1995]. One interpretation of this study is that reduced D2 presynaptic inhibition of ON terminals increases the odor responsiveness of mitral cells, but does so at the cost of reduced odorant discrimination.

GABA and $GABA_B$ receptors. $GABA_B$ receptors play a presynaptic inhibitory role, apparently very similar to that just described for D2 receptors. As noted above, GABAergic PG cells represent a large population of GL interneurons. In the rat MOB, the glomeruli have the highest concentration of $GABA_B$ receptors as determined by radioligand binding [Bowery et al., 1987; Chu et al., 1990] and by immunohistochemical localization of $GABA_B$ receptor subunits [Margeta-Mitrovic et al., 1999]. EM-immunohistochemistry revealed that the dense labeling in the GL is due to the presence of $GABA_B$ receptors on ON terminals and on the somata of PG cells [Bonino et al., 1999]. A variety of imaging and electrophysiological studies have provided solid evidence that GABA released from PG neurons presynaptically inhibits glutamate release from ON terminals via activation of these $GABA_B$ receptors [Aroniadou-Anderjaska et al., 2000; Keller et al., 1998; Murphy et al., 2005; Palouzier-Paulignan et al., 2002; Wachowiak and Cohen, 1999]. The presynaptic inhibition of glutamate release is mediated by suppression of Ca^{2+} influx into ON terminals [Wachowiak et al., 2005]. Stimulation of individual PG cells has been reported to inhibit, via $GABA_B$ receptors,

ON input onto the stimulated cell [Murphy et al., 2005]. The MOB also contains the highest levels of the putative inhibitory transmitter taurine, exceeding concentrations of GABA and glutamate [Collins, 1974; Margolis, 1974; Banay-Schwartz et al., 1989a,b; Ross et al., 1995; Kamisaki et al., 1996]. Taurine is found in ON axons, in various neurons, and in astrocytes [Kratskin et al., 2000; Kratskin and Belluzzi, 2002; Pow et al., 2002]. In the ON terminals and some postsynaptic dendrites, taurine is co-localized with glutamate [Didier et al., 1994]. In electrophysiological recordings, taurine directly activated presynaptic $GABA_B$ receptors and inhibited ON terminals, and it also induced chloride currents in mitral/tufted cells. Surprisingly, taurine had no direct effect on PG cells [Belluzzi et al., 2003].

9. SYNCHRONY AMONG JG CELLS

Synchrony can be defined as a meaningful temporal coincidence between two or more events that have a low probability of occurring by random or chance. Neurons involved in the detection and processing of odors show temporally correlated or synchronized activity, a feature that is expected to have functional relevance for understanding the population code in the olfactory system [Laurent, 2002].

The activity of JG neurons associated with the same glomerulus exhibit highly synchronous spontaneous activity. Simultaneous recordings of ET-PG or ET-SA cell pairs demonstrated that spikes in ET cells drive synchronous activity in PG and SA cells, but only if the dendrites of both cells ramified in the same glomerulus [Hayar et al., 2004b, Figure 3]. This intraglomerular synchronous activity is driven by glutamatergic input from ET cells to PG/SA cells and is abolished by AMPA receptor antagonists. Similar studies revealed that spontaneous spikes and subthreshold membrane potential activity (i.e., EPSPs, IPSPs) among ET cells of the same glomerulus is highly synchronous [Figure 3**;** Hayar et al., 2004b, 2005]. Interestingly, the frequency of spontaneous inhibitory input to ET cells, which primarily originates from PG cells, occurs around 50 Hz (within IPSC bursts) (gamma frequency) and is similar to the frequency of ON-evoked γ-oscillations in mitral cells (mean 45 Hz) [Lagier et al., 2004]. Although spontaneous synaptic input can synchronize ET cells, synchrony among these cells persists when ionotropic glutamate and GABA receptors are blocked [Hayar et al., 2004b, 2005]. Additional electrophysiological results demonstrated that ET cells of the same glomerulus are electrotonically-coupled via gap junctions with a relatively small conductance (0.1 nS). Spontaneous synchrony among ET cells is abolished by the gap junction blocker carbenoxolone [Hayar et al., 2005]. These results are consistent with anatomical evidence for gap junctions between mitral/tufted cell apical dendrites [Schoppa and Westbrook, 2002; Christie et al., 2005]. Unlike mitral cells, which exhibit a narrow window of spike-to-spike correlation [Schoppa and Westbrook, 2002], ET cells exhibit a broader window of burst-to-burst correlation. The narrow window of correlation among mitral cells is due to the fact that mitral cell spikes induced fast EPSPs in other mitral cells [Schoppa and Westbrook, 2002; Christie et al., 2005]. In contrast, ET cells seem to communicate mainly via slow inward currents produced by gap junctions with relatively low conductance. Therefore, one potential function of gap junctions in ET cells is to filter fast spiking activity and propagate slow membrane potential oscillations, which are driven mainly by persistent sodium currents [Hayar et al., 2004a]. Thus, the glomerulus comprises multiple means of communication,

which synchronize the glomerular ensemble and at the same time provide different rates of information transfer among JG cells (Figure 5).

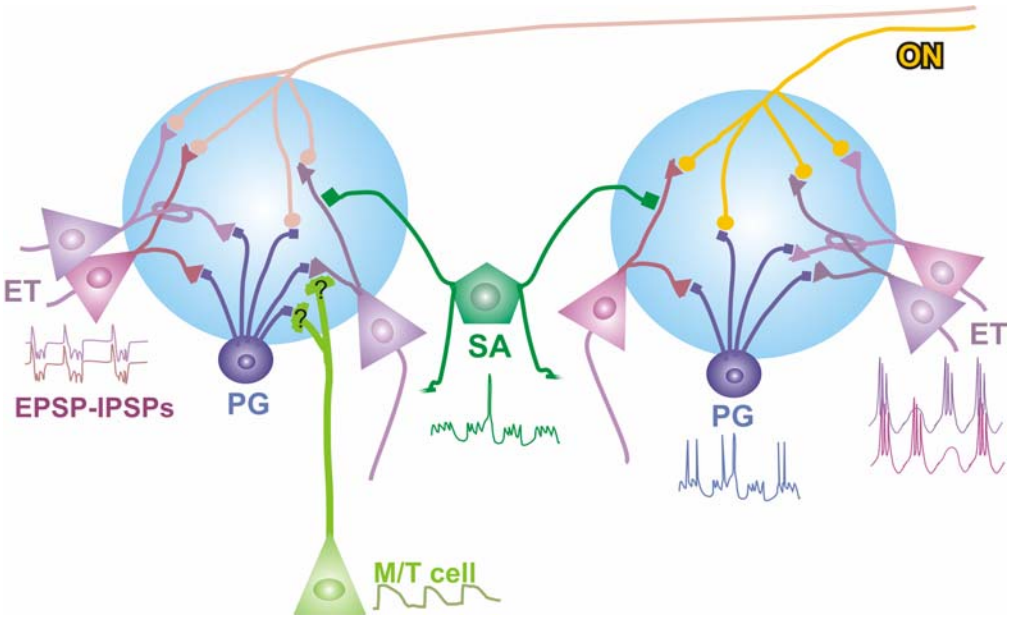

Figure 5. Schematic illustration of intra- and inter-glomerular circuitry. Glutamatergic ET cells rhythmically burst at sniffing frequencies and receive monosynaptic ON input. ET cells of the same glomerulus burst synchronously and trigger monosynaptic bursts of EPSPs in other JG interneurons (PG and SA cells), most of which do not receive direct ON input. ET cells are synchronized by ON input, glutamate spillover and interconnections via gap junctions (ovals). ET cells are also synchronized by IPSP bursts from the same and different sets of PG cells. PG cell dendrites ramify in a restricted portion of a single glomerulus and provide local intra-glomerular inhibition of ET cells via dendrodendritic interactions, and also exert presynaptic inhibition of ON terminals. By contrast, SA cells have dendrites and axons extending throughout several glomeruli, and thus might subserve interglomerular interactions. The synchronously bursting ET cell glomerular "ensemble" may constitute an oscillating rhythm generator that monosynaptically synchronizes the activity of PG cells within the same glomerulus, and perhaps also coordinates the activity of mitral/tufted cells via glutamate spillover.

Electron microscopic studies suggest an indirect coupling between mitral cells via intervening interneuronal processes in addition to the direct gap junction coupling between them [Kosaka and Kosaka, 2004]. These intervening processes originate from GABA-negative and TH- negative uncharacterized glomerular neurons that receive synapse from olfactory nerve terminals and are therefore likely to be the dendrites of ET cells [Kosaka and Kosaka, 2003]. Therefore, both ultrastructural and electrophysiological studies obtained so far indicate that mitral/tufted cells and ET cells might form gap junctions among themselves and among each other. One possible function of spike synchrony among ET and mitral cells would be promote the summation of EPSPs and the likelihood that cortical neurons fire action potentials in response to olfactory nerve input.

10. OSCILLATIONS AND THETA RHYTHM

Brain rhythms are thought to coordinate intra- and inter-structural communications, to play a role in temporal coding of sensory signals, in generation of memory traces, cognition and other mental activities. Oscillations and synchronous activity are characteristic features of spontaneous and odor-driven activity in the MOB [for reviews see Lledo et al., 2005; Gelperin, 2006; Kepecs et al., 2006]. Olfactory information is thought to be encoded, at least in part, by oscillating neural assemblies [Wehr and Laurent, 1996; Kauer, 1998; Kay and Laurent, 1999]. The inhalation of odor molecules has been reported to trigger oscillations in the olfactory bulb with different frequency ranges [reviewed by Lledo et al., 2005]. Robust fast oscillations defined by their frequencies as gamma (30–80 Hz) and beta (15–25 Hz), as well as slower ones called delta (1-3 Hz) and theta rhythms (3–12 Hz), are classically observed in the olfactory system. Whereas gamma and beta waves are induced by odor inputs, the delta and theta frequency band seems rather to be phase-locked with respiration.

Membrane as well as field potential oscillations are the result of complex interplay between synaptic and intrinsic phenomena. In the olfactory bulb, 2- to 12-Hz oscillations have been shown to follow the respiratory cycle with some deviations, and these oscillations are commonly called "theta" principally because they occupy a highly overlapping frequency band with hippocampal theta oscillations, although the band is broader than that defined as theta-frequency for neocortical and hippocampal electroencephalogram *in vivo* (3.5 Hz to 8 Hz) [Kay and Laurent, 1999; Kay, 2003, 2005]. Frequency of ET cells bursting ranges from ~1 to 8 Hz (mean 3.3 ± 0.18 bursts/s). This range overlaps with the delta-theta frequency range prominent in oscillatory neural activity in the rodent olfactory network, which are thought to be driven by sensory inputs during “passive” sniffing (1-3 Hz) as well as during “active” investigative sniffing (5-12 Hz) [Adrian, 1950; Welker, 1964; Macrides et al., 1982; Eeckman and Freeman, 1990; Kay and Laurent, 1999; Kay, 2003]. Sniffing is a rhythmic motor process essential for the acquisition of olfactory information. Electrophysiological studies-primarily from anesthetized rodents-demonstrated that olfactory neural responses are coupled to respiration [reviewed by Kepecs et al., 2006]. However, even when pushed to psychophysical limits using mixtures of two odors, rats needed to take only one sniff (<200 ms at theta frequency) to make a decision of maximum accuracy [Uchida and Mainen, 2003]. Therefore, for the purpose of odor quality discrimination, a fully refined olfactory sensory representation can emerge within a single sensorimotor theta cycle, suggesting that each sniff can be considered a snapshot of the olfactory world.

Studies using intracellular recordings from mitral cells in the mammalian olfactory bulb *in vivo* [Charpak et al., 2001; Luo and Katz, 2001; Margrie and Schaefer, 2003; Cang and Isaacson, 2003] show a dominating rhythm synchronized to the respiration cycle. This theta rhythm is dependent on nasal airflow, requires action potential generation/propagation and glutamatergic transmission within the olfactory bulb. Furthermore, the general kinetics of sensory input-evoked synaptic current in mitral cells is defined by the inspiration-exhalation cycle [Margrie and Schaefer, 2003].Odor application evoked an excitatory response characterized by synaptic depolarizations locked to the respiratory cycle, and on which were superimposed bursts of action potentials in the beta-gamma range [Wellis et al., 1989; Debarbieux et al., 2003].

11. INTRAGLOMERULAR OSCILLATOR EMERGES IN POPULATION ACTIVITY

The rhythmic firing patterns of ET cells in a glomerulus and the high correlation of their spontaneous membrane potential oscillations suggest that the synchronized spontaneous activity in the glomerular ensemble can generate local field potentials. Indeed, besides field potentials evoked by stimulation, there are readily detectable spontaneous field potentials of various amplitudes recorded in the glomerular layer (Figure 6, Figure 7 *A*, *B*). In interface slices of the rat MOB, patterns of rhythmic spontaneous field activity were found in some, but not in all recordings. Segments with distinctive regularity and duration not exceeding a few seconds were encountered only in 9 of 33 sites under normal conditions (Figure 6, horizontal bars, *B* central inset). The amplitude of regular oscillations was in the range of 0.018 to 0.194 mV (mean ± SE = 0.082 ± 0.002 mV, SD= 0.032 mV, n=127) and the frequency was in the delta-theta range (1-5 Hz). Presumably, these regular patterns reflect pure activity of the hypothesized cooperative intraglomerular pacemaker. However, in all cases regular oscillations were intermingled with dominating irregular events often of much higher amplitudes (Figure 6, marked with asterisks). Randomly emerging spontaneous field potentials indicate a sporadic involvement of a large number of neurons in the concomitant activity. These irregular events of various magnitudes were named spontaneous glomerular layer field potentials (sGLFPs) [Karnup et al., 2006].

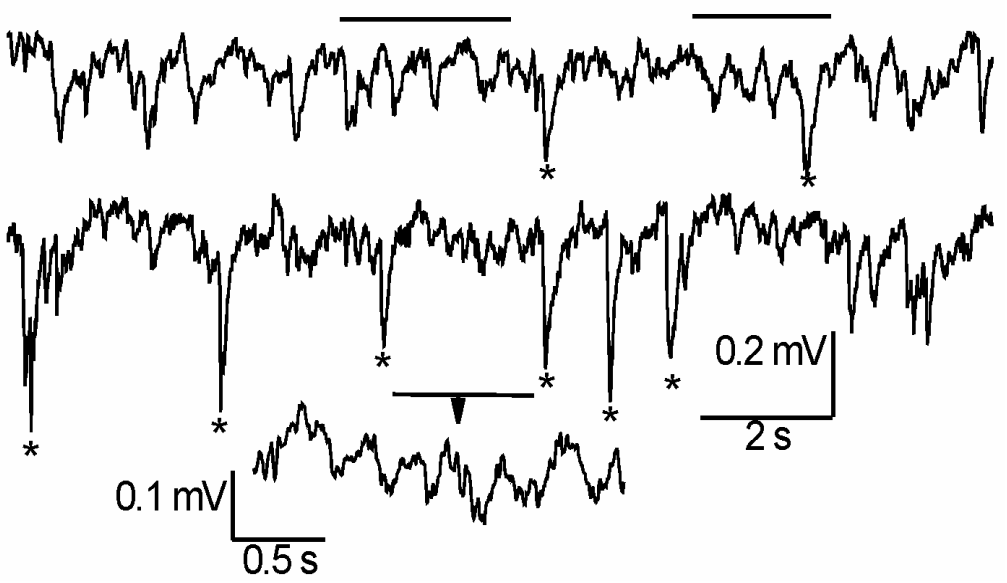

Figure 6. Patterns of rhythmic field potential oscillations in the glomerular layer. Lower trace was recorded in about a minute after the upper trace. Patterns of regular delta-oscillations (~1 Hz) are shown with horizontal bars above the upper trace. A pattern of theta-oscillations (~4 Hz) from the lower trace is shown in the inset. Large irregular spontaneous population events are marked by asterisks.

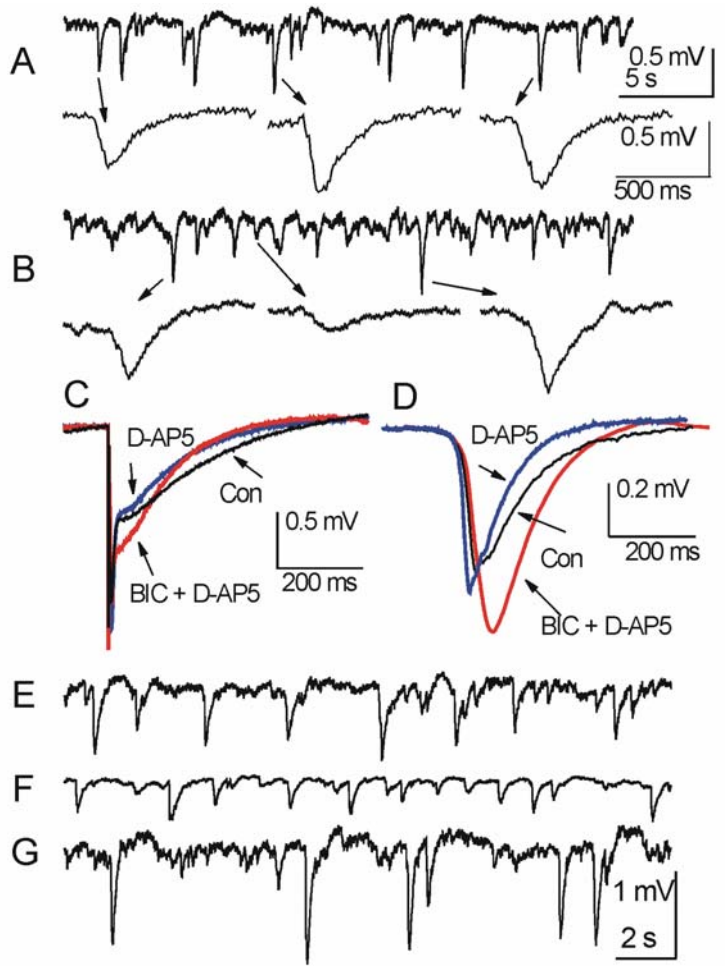

Figure 7. Spontaneous glomerular layer field potentials (sGLFPs). *A* and *B* – sGLFPs in two different control slices. Insets show some individual sGLFPs. Note various amplitudes and time courses of spontaneous events. *C* - averaged eFP (n=10) with stimulation at 100 μA. The fast early eFP phase emerges as an initial peak of ~20 ms duration and indicates occurrence of EPSPs synchronized by an input volley from ON. The following slow late eFP phase indicates development of recurrent excitation. *D* - averaged sGLFP from the same recording site (n=10, >90% of the maximal amplitude) displays similarity with the slow eFP in changes upon application of synaptic blockers. NMDA-receptor blocker D-AP5 shortened decay time and $GABA_A$-receptor blocker bicuculline (BIC) increased amplitudes in both sGLFP and late eFP phase to a similar extent. Note, that the late phase of the evoked field potential is comparable with sGLFP in the time course, amplitude and reaction to specific receptor blockers. Traces of sGLFPs in a control horizontal slice (*E)*, in a strip of isolated GL (*F*) and in a tangential slice (*G*). Somewhat lower sGLFP amplitudes in the glomerular strip are probably due to trauma while dissecting a 200 μm strip from a horizontal 400 μm thick slice. The frequency and amplitude of sGLFPs in tangential slices sometimes could exceed those in control slices.

12. COMMON MECHANISM OF EVOKED AND SPONTANEOUS POPULATION ACTIVITY IN THE GLOMERULAR LAYER

In conventional horizontal slices sGLFPs have negative polarity, which corresponds to excitation in neuronal populations (Figure 7 *A,B*) [Karnup et al., 2006]. sGLFPs were not all-or-none events as they varied considerably in amplitude, duration and shape. We considered an event as sGLFP if its amplitude exceeded 0.8 mV from its base, the steepest slope of the rising phase was less than 0.03 mV/ms, and its rise time (range 7 to 250 ms) was shorter than its decay time (range 30 to 600 ms). Despite qualitatively distinct appearance, sGLFPs did not fit to a standardized shape even in the same trace. Measured sGLFP parameters in all individual control recordings did not reveal clusters or any characteristic patterns. Neither individual, nor pooled data revealed correlation between the different parameters such as "half-width vs. amplitude" and "decay time vs. rise time". This indicates random recruitment of neurons into spontaneous population activity. We have previously shown that sGLFP is basically confined to a glomerulus of origin and does not propagate significantly to neighboring glomeruli (see below). Hence, the absence of a regular component in the majority of cases and its transient character when it is present, suggest that the intraglomerular pacemaker mechanism does not necessarily recruit the whole module into synchronized oscillations, but rather it works autonomously, and only occasionally it can trigger excitation in additional neurons.

The dendrites within the glomerulus were shown to be encapsulated by glial processes, separating the neuropil into compartments [Chao et al., 1997; Kasowski et al., 1999]. Diffusion of spilled glutamate and gap-junctions among dendrites [Kosaka et al., 2004; Christie et al., 2005; Hayar et al., 2005] are facilitated in a single compartment but prevented among compartments. Therefore, the glomerular compartment plays a role of a structural and functional subunit of a lower order than the entire glomerulus. A variety of kinetic properties of individual sGLFPs suggests that a spontaneous avalanche of excitation may be initiated in different intraglomerular compartments. Our data with intracellular recordings from astrocytes support this assumption (see below). Occurrence of random constellations of excited compartments may result in a variable number of cells involved in the sGLFP and in a continuum of its parameters.

The kinetics of large sGLFPs were strikingly similar to that of the late phase of evoked field potentials (eFP) produced by stimulation of the ON, suggesting that they may involve a common mechanism. In the case shown in Figure 7 *C,D* the largest (>90% of maximal amplitude) sGLFPs and slow component of eFPs evoked by moderate stimulation (up to half maximum) had identical durations, distributions of standard deviations and comparable amplitudes. The rapid rise time of the fast early phase of eFP is due to the synchronizing effect of the olfactory nerve activation. Thus, all stimulus-synchronized cellular voltage changes, including EPSPs and calcium spikes (McQuiston and Katz, 2001), may contribute to this fast population event. The slower kinetics of the late eFP phase and sGLFP were probably due to a gradual engagement of postsynaptic neurons, producing an avalanche of intraglomerular transmitter release. The possibility of a common mechanism generating both the sGLFP and the late phase of eFP is supported by the similarity of sGLFP and eFP decay course, by the occlusion of sGLFPs after eFP, and by the reduction of the late eFP when the stimulus was given during largest sGLFP [Karnup et al., 2006]. Stimulation in the ONL could

elicit eFP of much greater amplitude than that of largest sGLFP at the same site, which is probably due to synchronized activation of many neighboring glomeruli upon electrical stimulation and synchronous engagement of corresponding M/T cells. In the case shown in Figure 7, a maximal eFP could reach 4 mV (Figure 7*C,* black), whereas the largest sGLFPs at the same site were only ~1.8 mV (Figure 7*D*, black). On average, the ratio $sGLFP_{max}/eFP_{max}$ in horizontal slices in normal artificial cerebrospinal fluid (ACSF) was 0.27±0.04 (n=16, one recording site per slice). Upon blockade of $GABA_A$ receptors by bicuculline (BIC) the $sGLFP_{max}/eFP_{max}$ ratio increased from 0.27±0.04 (n=16) to 0.51±0.11 (n=5). The amplitude ratio 1:2 in the absence of inhibition suggests one of two options. First, if both evoked and spontaneous field potentials are generated only by the recorded module, then only half of its neurons can participate in cooperative spontaneous activity. Second, if eFP represents a sum of synchronized potentials from a few (or many) modules, and if sGLFPs in neighboring glomeruli are not synchronized, then about half of eFP is produced in the recorded glomerulus and another half is contributed by adjacent modules. Considering the limited sGLFP propagation beyond the glomerular shell, the absence or poor correlation among sGLFPs in adjacent glomeruli [Karnup et al., 2006] and the fact of synchronous involvement of many modules into evoked activity, the second option is more likely to be the case. Finally, blockade of AMPA-R by CNQX completely abolished both evoked and spontaneous field potentials. This confirms that excitatory interactions, which give rise to population events in the GL, are mediated by glutamate AMPA receptors [Karnup et al., 2006].

Self-sufficiency of the glomerular layer for production of sGLFP was shown in slices of the isolated GL. Spontaneous GLFPs, recorded from glomerular strip preparations (Figure 7, F) and from the GL in tangential slices (Figure 6, G), were comparable to those recorded in control slices (Figure 7, E). Thus, experiments with surgically isolated glomerular layer resulted in two main findings. First, M/T cells do contribute, but only weakly, to sGLFP generation. Second, mitral and tufted cells are not the only types of neurons responsible for sGLFP generation. Similar sGLFP magnitudes in the isolated GL and in control slices suggest that JG cells are the major contributors to spontaneous population events in the GL of acute MOB slices.

13. Delayed Involvement of Mitral Cells in the Glomerular Spontaneous Activity

Despite the fact that sGLFPs can originate in the GL due to recurrent excitation within glomeruli, in the intact olfactory bulb or in the control horizontal slice, these local population events additionally involve output M/T cells. Furthermore, sGLFPs may represent population events correlated with mitral cell spontaneous long-lasting depolarizations (sLLDs) [Carlson et al., 2000], which are also AMPA-R-mediated. To investigate the relationship between sGLFPs and sLLDs, we performed whole-cell recording from a mitral cell and field potential recording from the glomerulus containing its tuft [Karnup et al., 2006]. Correspondence between intracellular membrane potential and field potential recordings was established by the systematic presence of synchronized voltage deflections in both traces and the lack of such synchronized events when the sGLFPs were recorded in adjacent glomeruli (in each field recording 3 electrodes were placed in 3 neighboring glomeruli). In such dual recordings,

every sLLD had a concomitant sGLFP (Figure 8*A*). The amplitude and shape of these sGLFPs varied substantially, indicating that although a given mitral cell was involved in every event, the constellation of neurons recruited in each sGLFP was variable. Individual sGLFP frequently had shorter rise time, shorter duration, earlier onset, and typically reached the peak earlier than simultaneously recorded sLLDs (Figure 7*A* insets). With the reference point set at the sLLD onset in three of five dual recordings, the onset of the averaged sGLFP preceded that of sLLD by ~10 ms (Figure 8*B*).

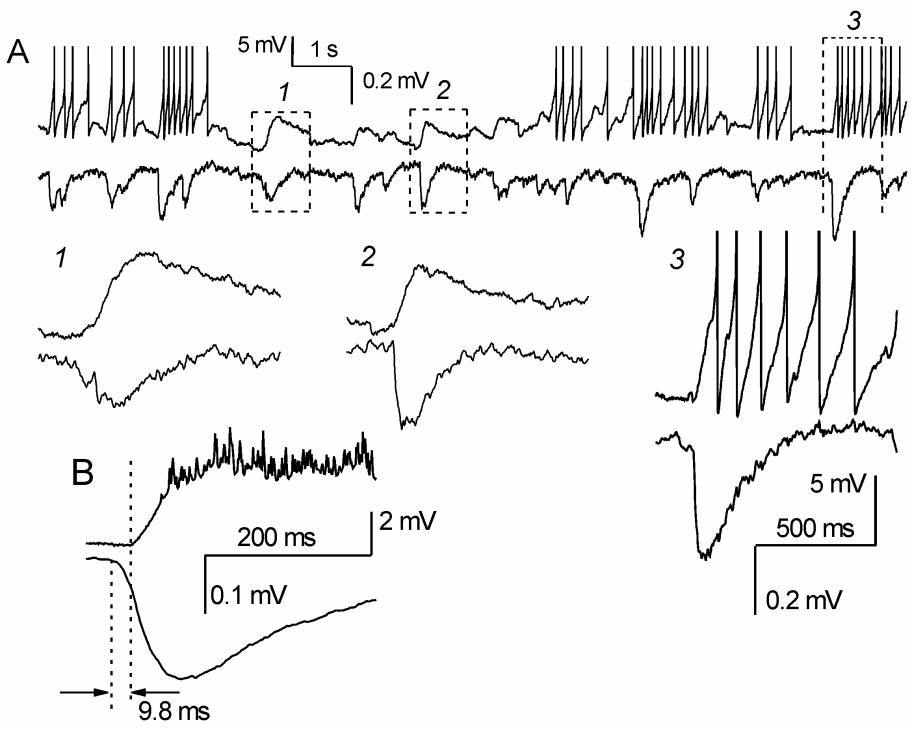

Figure 8. Interactions between a glomerular pool of JG cells and a mitral cell. *A* - simultaneous recordings of sLLDs in a mitral cell (upper trace) and sGLFPs (lower trace) from a glomerulus containing the mitral cell tuft. Spikes of mitral cell are truncated. Insets with an expanded time scale demonstrate variability of sGLFP locked to sLLD and different kinetics of sGLFP as compared to sLLD. *B* – averaged sLLD and sGLFP (n=80) with the reference point set at the sLLD onset show 9.8 ms delay of sLLD upon initiation of sGLFP, thus indicating leading role of JG cell pool in activation of the module.

Furthermore, sLLD-induced mitral cell spikes were delayed on average by 50 ms from the sGLFP onset; therefore, spike-dependent glutamate release from mitral cell tuft at best could contribute to sGLFP after it reached 90%-100% of its peak (Figure 8*A inset 3, B*). This finding implies that M/T cells are not necessarily initiators of spontaneous intraglomerular excitation, but on the contrary they may be either followers or equal participants of the population event. Thus, a time lag in correlation between sLLDs and sGLFPs is in agreement with the notion of self-sufficiency of the JG ensemble in producing sGLFPs and with the idea that JG ensembles lead the information processing.

14. GLIAL CELLS AS INTRAGLOMERULAR PROBES

A more direct proof of sGLFP initiation by spontaneous activation of JG cells could be obtained by simultaneous intracellular recording of a JG cell and an extracellular field potential from the same glomerulus. However, in the interface slice, where sGLFPs are well pronounced, obtaining a blind whole-cell recording from JG cells turned out to be difficult. In submerged slices, where JG cells can be readily patched, eFPs are hardly detectable and spontaneous events of smaller amplitude are indistinguishable from the noise level. To overcome this problem we took advantage of the fact that intraglomerular glial cells can serve as indicators of intraglomerular neuronal activity. Astrocytes in the GL have small somata comparable to that of PG cells (~5-10 μm), exhibit dense spongiform ramifications extending from major processes, and project their processes into the core of a single glomerulus [Chao et al, 1997; De Saint Jan and Westbrook, 2005; Bailey and Shipley, 1993]. In the submerged slice, ONL stimulation elicits synchronized depolarizing membrane potentials both in a glial and a mitral cell associated with the same glomerulus [De Saint Jan and Westbrook, 2005]. The authors have shown that glial response to ON stimulation consists of two components. The first component consists of a fast and short initial inward current induced by a synaptically-activated glutamate transporter current (amplitude 128 ± 20 pA, 10-90% rise time of 5.2 ± 0.3 ms (n=20) and half-width ~25-30 ms), which corresponds to glutamate clearance from the extracellular space. The second component of the glial response represents a slowly decaying inward current with an amplitude and duration increasing with stimulus strength. At half-maximal stimulation by a single shock (~50 V, Δt=0.1 ms) the total evoked current in rat astrocytes had a half-width of 1108 ± 154 ms and an amplitude of 232 ± 20 pA (n=27). Since the slow second component was effectively blocked by barium (100-200 μM), it was ascribed to the inward rectifier K^+ channels. These channels play a role in spatial buffering of K^+ released in the extracellular space during neuronal activity [Karwoski et al., 1989; Newman, 1993; Kofuji and Neuman, 2004]. Since olfactory nerve terminals release only a small fraction of total K^+, most of the K^+ released in glomeruli after olfactory nerve stimulation originates from postsynaptic spiking cells [Jahr and Nicoll, 1981; Khayari et al., 1988], and during spontaneous activity all of the increase in extracellular K^+ is due to neuronal firing. Blockade of ionotropic and metabotropic glutamate receptors led to complete elimination of evoked potentials in mitral cells and a substantial reduction of the evoked current in glial cells. This suggested that the K^+ component of the astrocyte response essentially reflects electrical activity of neurons having dendrites in a given glomerulus (De Saint Jan and Westbrook, 2005). This K^+-mediated slow depolarization in a glial cell will be further referred to as a glial potassium potential (GPP), which can be either evoked (eGPP) or spontaneous (sGPP).

The glial cells of the glomerular layer in our experiments were distinguished from neurons by low membrane potentials (-79.6 ± 0.8 mV, SD=5.2, n=45), low input resistance (106 ± 11, SD=57, n=23), linear I/V characteristic and inability to generate spikes. Two glial cells were obtained blindly in the interface mode and 43 cells were patched in the submerged mode under visual control. In the interface mode, we simultaneously recorded field potentials in the GL with a regular ACSF-filled pipette and membrane potentials of astrocytes using sharp electrodes (Figure 9 *A*).

Although the pipette and the sharp electrode were positioned in close vicinity, this did not guarantee association of an astrocyte with the recorded glomerulus. However, since many adjacent modules were synchronously activated, the response (i.e. eGPP) in the astrocyte must be synchronized with any of them.

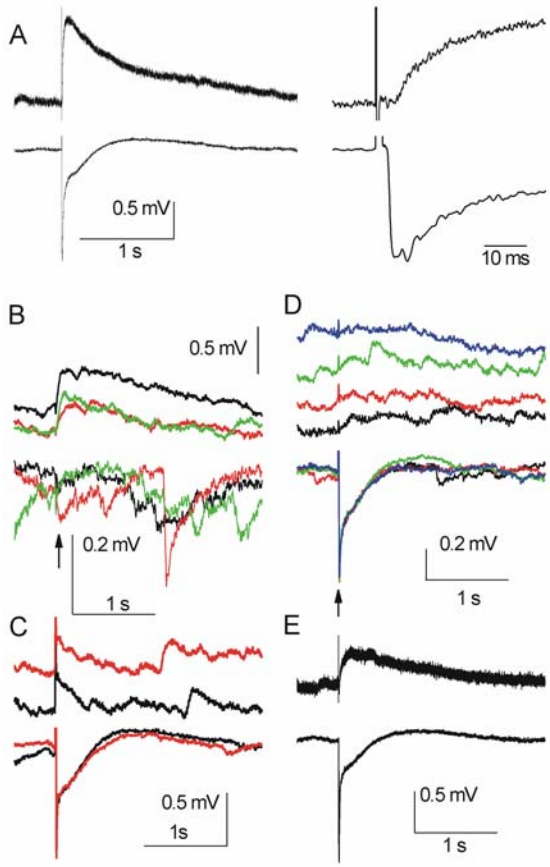

Figure 9. Dual recordings of field potentials (lower traces) and an astrocyte (upper traces). *A* - Averaged (n=5) evoked responses (on the left) to half-maximal stimulation in the ONL (50 μA) show longer duration of the astrocyte depolarization as compared to the field potential. Latency of the astrocyte response (4.9 ms) was also longer than that of the eFP (2.6 ms) (right panels with the expanded time scale). *B* – ONL stimulation with the intensity slightly subthreshold (5.5 μA for the astrocyte response). Note failures of the eFP (lower green trace) whereas sGLFPs were well pronounced (all upper traces). *C* - Stimulation in the EPL (100 μA, two-fold threshold intensity for the astrocyte response). Despite a well-expressed late phase of this eFP, which was greater than eFP during ONL stimulation, glial depolarization was weaker. Glial response did not reveal a detectable latency. Note spontaneous depolarizing events in the astrocyte with kinetics similar to evoked responses and lack of their counterparts in the field traces. *D* – Stimulation from an adjacent glomerulus (150 μm away from the astrocyte in the caudal direction) at threshold intensity for the astrocyte (20 μA) evoked a pronounced eFP accompanied by frequent failures in the astrocyte. *E* – Averaged responses (n=5) to a slightly stronger stimulation (25mA) from the same site in the GL demonstrate 9% increase in eFP and significant depolarization in the astrocyte (peak amplitude 0.42 mV). The latency of the astrocyte response was substantially longer than that of eFP (11.5 ms and 1.2 ms correspondingly). It is likely that ONL stimulation in *B* delivered an input precisely to the compartment created by the astrocyte, whereas GL stimulation in *D* activated (through SA cells) most of the glomerular population except for the compartment of the recorded astrocyte. In *B* and *D* voltage scales for glial responses are the same, whereas voltage scales for eFP are different; arrows designate stimulation.

The averaged (n=5) evoked responses induced by half-maximal stimulation in the ONL (50 μA) (Fig 8 *A*, on the left) demonstrate longer duration of the astrocyte depolarization (half-width 600 ms, total duration 3 s) as compared to the field potential (half-width 200 ms, total duration 920 ms) indicating that the extracellular K^+ concentration increased long after intraglomerular excitation was terminated. The latency of the astrocyte eGPP (4.9 ms) is also longer than that of the eFP (2.6 ms) (Figure 9 *A*, right panels).

The difference between the latencies may be due to the time necessary for K^+ diffusion from neuronal dendrites to glial cell processes. Stimulation from other sites revealed a different sensitivity of this glial cell to different inputs and a lack of direct correspondence of its responses to the average level of excitation in the glomerulus. Upon ONL stimulation with intensity slightly superthreshold for eGPP (5.5 μA) the eFPs were inconsistent and had occasional failures, although sGLFPs were well pronounced (Figure 9 *B*). In this case a few activated ON fibers might reliably activate dendrites in a compartment associated with the recorded astrocyte, whereas the majority of neurons did not receive or received input with occasional failures. The eFP was well expressed and steady when stimulation with two-fold threshold intensity for the field response (100 μA) was made from the lower EPL (Figure 9 *C,* lower traces). Here the late phase of eFP was greater than that upon ONL stimulation in *A* (amplitude of the late phase 0.48 mV in *C* and 0.28 mV in *A,* lower traces), whereas glial depolarization was weaker (0.36 mV and 1.2 mV correspondingly, Figure 9 *C* and *A* upper traces). Higher eFP amplitude and lack of detectable latency in the glial response in *C* might be due to direct stimulation of M/T cells, whose dendritic tufts were in direct contact with the astrocyte, but other neurons contacting the astrocyte did not generate spikes. Stimulation from an adjacent glomerulus (150 μm away from the astrocyte in the caudal direction) at threshold intensity for the astrocyte (20 μA) evoked a pronounced eFP (amplitude of the late phase 0.34 mV), but the astrocyte in most cases failed to respond (Figure 9, *D*). This suggests that excitatory inputs were delivered through interglomerular connections (see below) to most of the glomerulus population except for the compartment of the recorded astrocyte. The averaged response to a slightly stronger stimulation (25 μA, n=5) from this site in the GL demonstrates ~9% increase in eFP (latency 1.2 ms, late phase 0.37 mV) and sharply emerging depolarization in the astrocyte (latency 11.5 ms, peak amplitude 0.42 mV) indicating engagement of neurons in its area of control. The difference of latencies between field and glial responses to GL stimulation was even greater than that after moderate ONL stimulation (10.3 ms and 2.3 ms, correspondingly). This might be due to a longer distance for K^+ to diffuse or due to a few synaptic delays before excitation reached the astrocyte's compartment. Taken together the results in Figure 9 *B-E* suggest that the given astrocyte selectively responded to neuronal activation only in some glomerular compartments, but not any neuronal activation within the glomerulus caused its response.

Out of 45 astrocytes responding to ON stimulation, 28 did not show spontaneous depolarizations. Nevertheless, 17 glial cells (16 of them in submerged slices) did show sGPP with patterns similar to those of sGLFPs (Figure 10). Typically, their maximal amplitude was lower than that of the moderate evoked response. It is likely that sGPPs of large amplitude similar to eGPP (compare Figure 10 *Ba* and *A* upper trace) mirrored synchronized excitation of large neuronal populations, whereas small sGPPs might reflect activation of a few neurons or even a single neuron. On average, (n=194) sGPP parameters were: amplitude M ±SE = 0.187 ± 0.013 mV, SD=0.181 mV, range from 0.003 to 1.125 mV; half-width 190.6 ± 7.6 ms,

SD=105.8 ms, range from 53 to 771 ms; 0% to 100% rise time 96.3 ± 4.1 ms, SD=57.2 ms, range from 23 to 352 ms. Random occurrence and superimposition of sGPPs (Figure 10, *Bb* insets) are similar to that of sGLFPs. All processes of an astrocyte are confined to a single glomerulus (Bailey and Shipley, 1993); hence, all sGPPs follow neuronal excitation exclusively in a given glomerulus. The similarity between sGPP and sGLFP patterns confirms the assumption that sGLFPs of various amplitudes can be generated in the same glomerulus but in different compartments or different constellations of compartments.

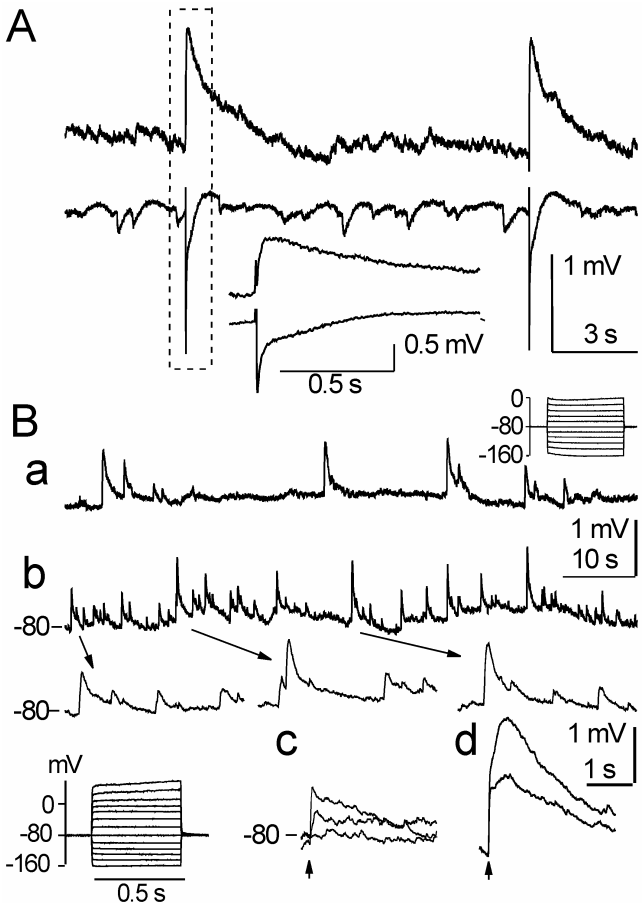

Figure 10. *A* - Dual recordings of field potentials and an astrocyte. Stimulation of the olfactory nerve at half-maximum intensity (50 μA, Δt=0.2 ms) elicited synchronized evoked responses in the individual astrocyte (top trace) and in the surrounding neuronal population (bottom trace). The inset shows a pair of responses (dashed box) with the expanded time scale. There were non-coinciding spontaneous events between evoked responses in both traces. *B a,b* – whole-cell recordings with spontaneous depolarizations from two glial cells in submerged slices. Insets in *b* show multiple overlapping evoked potentials in the glial cell, presumably occurring in different processes of the astrocyte involved in a few intraglomerular compartments; insets with current injections from -500pA to +500pA to the astrocyte *a* and from -600 pA to +700 pA (100 pA increment) to the astrocyte *b* show linearity of the I/V characteristics; *c* – stimulation in the ONL at threshold intensity (20 μA) elicited responses similar to spontaneous depolarizations; *d* - strong stimulation (200 μA, two different polarities) evoked maximal response lasting for 3 to 5 s.

Apparently, they can occasionally synchronize to form large glomerular field potentials involving most of the glomerular ensemble. Interestingly, in two occasions we observed fragments of theta-oscillations (4-5 Hz) in an astrocyte, which was probably in contact with rhythmically busting ET cells (not shown). The sensitivity of astrocytes to activation of small neuronal subpopulations in the glomerular module gives an opportunity to use sGPP as a tool to study the fine intraglomerular organization and its functional compartmentalization.

15. THE NETWORK OF SHORT-AXON CELLS IS THE BASIS FOR INTERGLOMERULAR COMMUNICATION

Until recently glomeruli of the MOB were considered as poorly communicating structural units, because in classical Golgi and degeneration studies axonal projections of JG cells were reported to extend only 1-3 glomeruli from the cell soma [Cajal, 1911b; Golgi, 1875; Pinching and Powell, 1971a, 1971b, 1972b]. However, as the Golgi-Cox method stains axons incompletely, the classical approach underestimated the extent of axonal arborizations in the GL. In labeling experiments with DiI, microbeads and biocytin, we have shown that there is a type of local neurons whose long axons provide ample interglomerular connections spanning distances up to 2 mm (20-30 glomeruli radii) (Aungst et al., 2003). These long axons actually belong to "short axon" (SA) cells, which were well characterized morphologically in classical studies except for the length and richness of their axonal trajectories. In contrast to ET and PG cells, they are not associated with a particular glomerulus and do not have dendritic tufts. A few (3-5) poorly branched dendrites of SA cells have random orientation in the interglomerular space, extend for up to 3-4 glomeruli from the soma and can penetrate into the glomerular neuropil. The greater extent of axonal arborizations as shown in biocytin-filled SA cells (Figure 11 *C*) versus that seen in classical studies is probably due to the limited impregnation of axons achieved with the Golgi-Cox method [Cajal, 1911b; Pinching and Powell, 1972b].

To estimate the density and area of neuronal processes propagation within the glomerular layer, a single subglomerular iontophoretic microinjection (5-10 μm diameter) of the lipophylic tracer DiI was made in the tangential "surface" slice. This type of slice was made from a medial surface of the rat or mouse MOB and it contained the ONL, GL and a part of EPL. As soon as DiI is taken up by the cell's membrane it diffuses over the entire cell including all processes and the soma. Analysis of labeled JG cell distribution showed that 50% of labeled cell bodies were located at distances greater than 350 μm (~5-7 glomeruli) from the injection site, and 10% were located at distances greater than 850 μm (~15-20 glomeruli) (Figure 11, *A*) [Aungst et a., 2003]. As DiI is captured by all membranes and undergoes both anteretrograde and retrograde transport, we used also rhodamine microbeads - a retrograde tracer taken up preferentially at synaptic endings [Cornwall and Phyllipson, 1988] – which were injected into the glomerular layer *in vivo* to confirm the anatomical results. The distribution of microbead-labeled cells from a single injection in each animal was similar to that seen with DiI, suggesting long and profound axonal, rather than dendritic projections from SA cells. Since all microinjections were smaller than the diameter of a glomerulus (5-10 μm vs. 50-100 μm), these results underestimate the number of cells

innervating a single glomerulus. However, they show that interglomerular connections extend over much greater distances than it was previously thought.

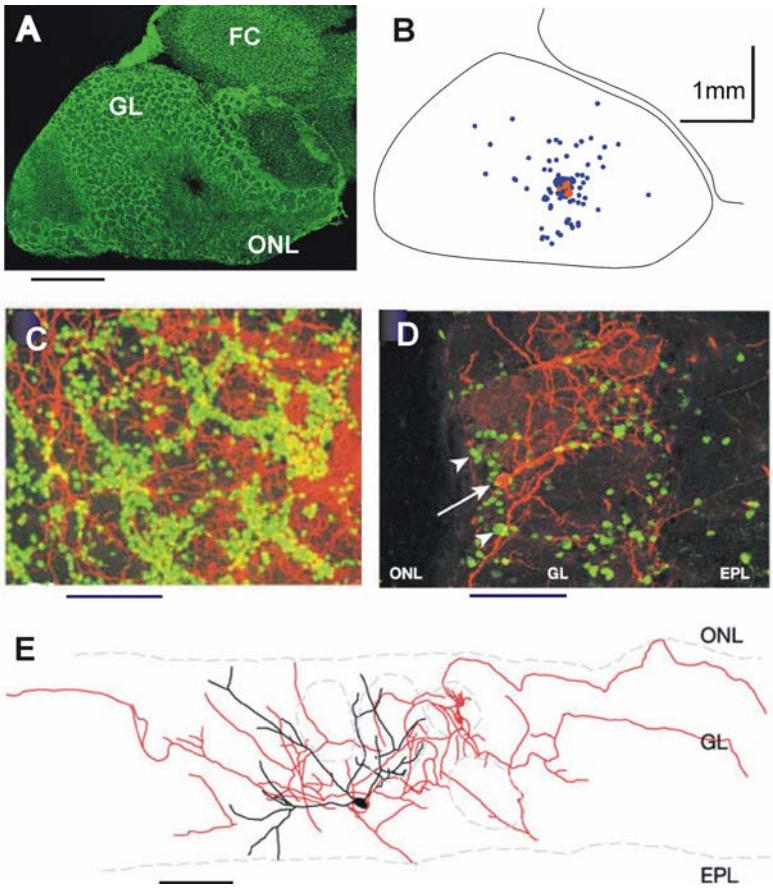

Figure 11. *A* - Tangential slice of the medial surface of the MOB with a nuclear counterstain (green). Glomerular layer (GL) and olfactory nerve layer (ONL) are visible in the same plane; FC – frontal cortex. *B* – Distribution of all labeled JG cells (cell bodies – blue dots, injection site – red dot) after a single subglomerular-sized injection of DiI in the tangential slice shown in *A*. *C* – DiI-labeled processes form a dense plexus both in the extra- and intraglomerular space (injection site is off panel). *D* – subpopulation of GAD65-GFP expressing PG cells (green, arrowheads) outlines glomerular shells. GFP-negative but DiI-labeled SA neuron (arrow, injection site is 350 μm away) demonstrates, that SA cells are non-GABAergic neurons. *D* - Reconstruction of a biocytin-filled SA cell (dendrites – black, axon – red). Scale bars represent 1 mm in *A* and *B*, 100 μm in *C*-*E*.

It has been generally thought that interglomerular connections are inhibitory and derive from GABAergic PG cells. It is partly true, because some PG cells have short axons reaching 1-3 glomeruli from the soma [Pinching and Powell, 1971a]. This explains monosynaptic IPSPs at short distances (see below). However, SA cells, providing long-distance communications, turned out to be non-GABAergic [Aungst et al., 2003]. DiI injections in the transgenic mice in which the promoter for GAD65 (glutamic acid decarboxylase 65, the principal GABA-synthesizing enzyme in the MOB) drives the expression of green fluorescent protein (GFP), gave the same distribution of labeled cells as in wild-type mice and in rats. Only ~9% of DiI labeled cells located one, two or three glomeruli from injection sites

contained GFP, indicating that they were GABAergic neurons. Other ~91% of DiI labeled cells did not show co-localization of red and green fluorescence, indicating that they are probably glutamatergic cells. Therefore, the contribution of GABAergic cells to interglomerular connections is minor and they seem to provide inhibitory inputs only to the immediate neighborhood of a central glomerulus. Thus, we can conclude that the population of SA cells forms a morphological substrate for connecting the GL to actively interacting subsystem of glomerular modules.

16. INTERGOMERULAR CONNECTIONS ARE PREDOMINANTLY EXCITATORY

To investigate whether the interglomerular interactions are excitatory or inhibitory, whole-cell recordings were made from JG cells, 2 - 4 glomeruli away from the site of focal stimulation in the GL of horizontal slices (Figure 12 A).

The ONL was cut between the stimulation and recording site to prevent propagation of the stimulus through olfactory nerve fibers. From a total of 58 JG cells tested with GL stimulation, 41 cells were PG, 15 ET and 2 SA. All cells were identified according to morphological criteria [Pinching and Powell, 1971a; Cajal, 1911b; Golgi, 1875]. Stimulus intensity was in the range of 100-500 μA (stronger currents caused tissue damage). Only 44% (26 of 59) JG cells responded to stimulation with either EPSPs or IPSPs. In some neurons a change in stimulus polarity led to conversion of monosynaptic responses to polysynaptic or vice versa (5 cells). Responses were obtained in 45% (19 of 42) PG cells, 40% (6 of 9) ET cells and 50% (1 of 2) SA cells. In most of responding cells distant GL stimulation elicited EPSPs (Figure 12 B, C, D).

Namely, 63% (12 of 19) PG, 83% (5 of 6) ET and one of two SA cells were excited through interglomerular connections. From 12 PG cells responding with EPSP 6 had only monosynaptic EPSP (latency 1.69 ± 0.16 ms), 4 had only polysynaptic EPSPs and 2 PG cells had both monosynaptic and polysynaptic responses depending on polarity of stimulation. The averaged latency of polysynaptic EPSP in PG cells was 7.4 ± 1.2 ms (SD=3.0 ms, n=6). The excitatory responses in 5 ET cells were monosynaptic (latency 2.0 ± 0.3 ms); one of these ET cells showed polysynaptic EPSPs (latency 3.1- 4.8 ms) after change of stimulus polarity. One of the two tested SA cells responded to GL stimulation with polysynaptic EPSPs (latency 5.3 ± 0.6 ms, range 3.8 – 7.9 ms, n=13).

Excitatory nature of interglomerular connections is further supported by *in vitro* experiments with a voltage-sensitive dye RH414 [Aungst et al., 2003]. Tangential slice of the medial MOB surface (a sheet containing only GL and ONL) was loaded with the dye. Focal stimulation (n=6 slices) evoked wide spread depolarization lasting ~200 ms. Depolarization propagated in all directions from a stimulation site for ~ 1 mm. This wide spread depolarizing response was completely and reversibly abolished by blockade of ionotropic glutamate receptors with CNQX and APV. These results indicate that interglomerular connections are extensive, excitatory and mediated by glutamate acting at ionotropic receptors.

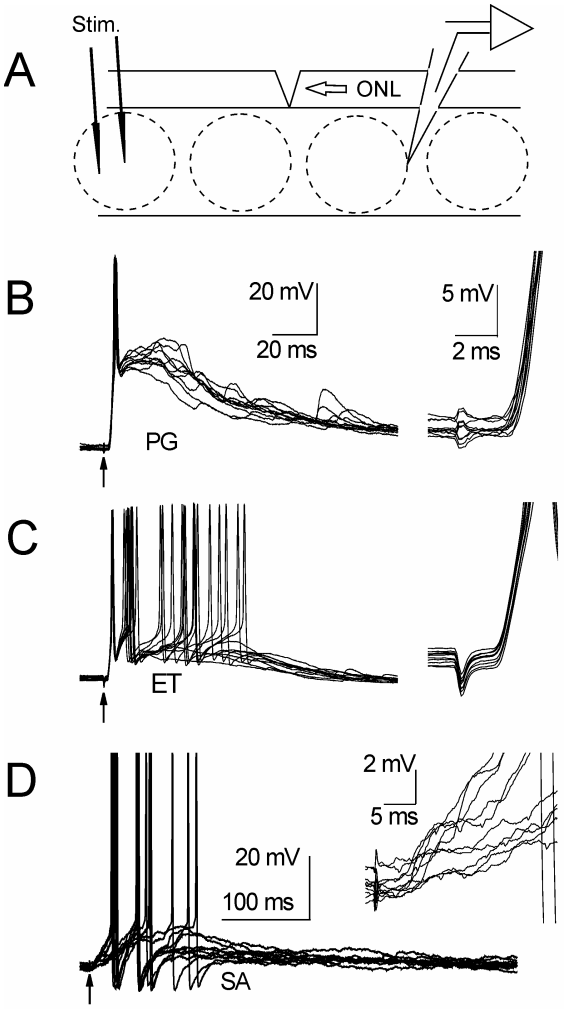

Figure 12. Responses of JG cells to remote electrical stimulation in the GL. *A* – Diagram of electrode locations. ONL was cut between stimulation and recording sites to avoid antidromic excitation of the receptor cell axons. The hollow arrow in the ONL designates rostro-caudal direction. Recorded cells and stimulation site were separated by 1 to 3 glomeruli. *B* – monosynaptic EPSP in a PG cell (latency 2.05 ± 0.05 ms, n=10; inset on the right) elicited a single spike followed by a plateau-potential. *C* – monosynaptic EPSP in the ET cell (latency 1.52 ± 0.01 ms, n=38; inset on the right) elicited a burst of spikes. *D* - SA cell responded with polysynaptic EPSPs (latencies 5.1 ± 0.6, (n=7) and 5.9 ± 0.6 (n=5) at different polarities of stimulation). Scales in *B* and *C* are the same.

17. INTERGLOMERULAR INHIBITION

In addition to excitatory connections, intra-GL stimulation revealed feedforward and feedback lateral inhibition at distances of 2-3 glomeruli. Feedforward inhibition is likely to occur via axons of GABAergic PG cells. The axons of PG cells are rare, but in the whole bulb they have been reported to extend over distances equivalent to 4-5 glomeruli [Blanes, 1898; Pinching and Powell, 1971a]. In slices we saw PG axons spanning only 1-2 glomeruli [Hayar et al., 2004a]. The inhibitory input can be powerful enough to prevent EPSPs and firing in

postsynaptic cells. Figure 13 demonstrates that spontaneous activity of the PG cell was only slightly distorted by stimuli just suprathreshold for IPSP generation, but strong stimulation interrupted a barrage of spontaneous EPSPs. This was likely to be a monosynaptic inhibitory input with a small jitter (latency 3.88 ± 0.02 ms, SD=0.12, n=37) originating from directly-stimulated PG cells located two glomeruli away. In our experiments 7 PG cells responded with monosynaptic IPSP (latency 3.29 ± 0.35 ms) and 2 of them showed polysynaptic IPSP upon change of stimulation polarity (latency 3.2 - 6.4 ms and 4.8 – 8.2 ms). One of five responding ET cells had only an initial IPSP (latency 3.1 ms) and did not reveal an excitatory postsynaptic potential. Interestingly, all neurons responding to GL stimulation showed either eEPSP or eIPSP, but not a sequence of EPSP-IPSP as it is typical for other structures [Karnup and Stelzer, 1999].

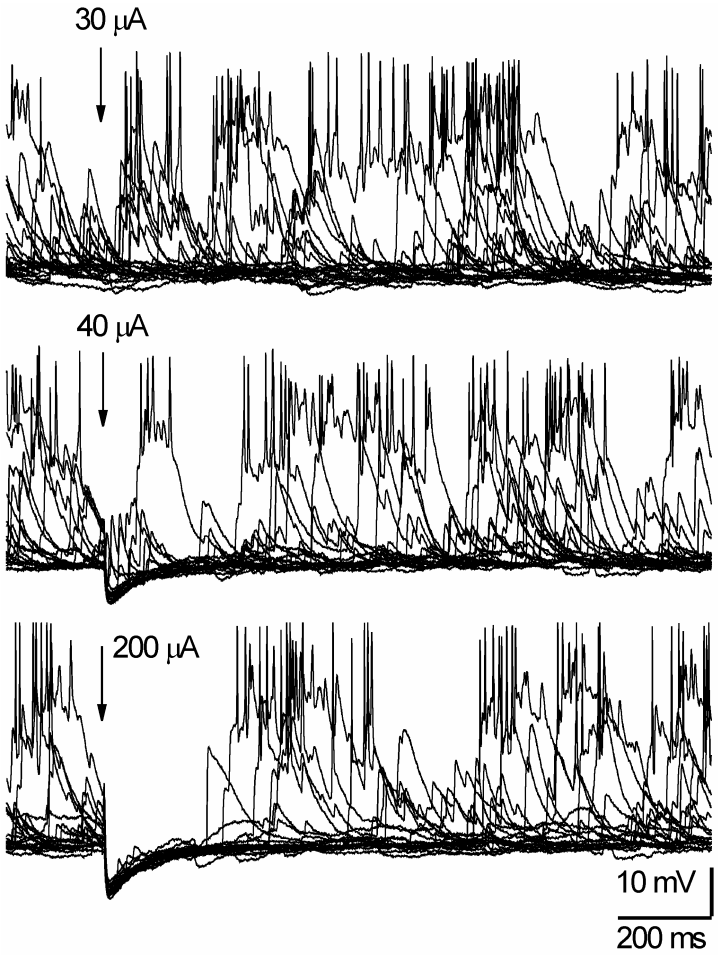

Figure 13. IPSPs in the PG cell elicited at different intensities of remote stimulation in the GL. Despite a rather long duration of latency it had a very small jitter, which suggests a monosynaptic transmission (3.88 ± 0.02 ms, n=37). Recording and stimulation sites were separated by 2 glomeruli. Threshold (30 μA, upper traces) and slightly superthreshold (40 μA, middle traces) stimulation did not prevent bursts of spontaneous EPSPs in the PG cell. Strong stimulation (200 μA, lower traces) blocked spontaneous EPSPs, indicating either feedforward or feedback lateral inhibition in a given glomerulus.

However, it was recently shown [Figure 3 of Hayar et al., 2005] that ET cells do receive spontaneous and ON-evoked EPSC followed by IPSC burst that most likely result from PG cell feedback inhibition. Therefore, it is possible that only an excitatory input originating from ON, but not from GL, produces an EPSP-IPSP sequence in ET cells. Lateral feedforward or feedback inhibition might depend on stimulation strength. With moderate GL-stimulation the majority of responding JG cells (69%, 18 of 26 [12 PG, 5 ET and 1 SA cells]) displayed mono- or polysynaptic EPSP and only two PG cells had input-dependent polysynaptic IPSPs, presumably mediated by SA-to-PG synaptic transmission. In the remaining JG cells, (31%, 8 of 26 [7 PG and 1 ET cells]) GL-stimulation evoked monosynaptic IPSPs, presumably from direct stimulation of PG cells. Therefore, we conclude that at moderate stimulation intensities the SA-mediated excitation of distant modules does not reach a threshold to trigger feedback inhibition in these modules. It rather somewhat increases excitability in a surrounding area. On the contrary, these stimulation intensities are sufficient to deliver IPSPs to adjacent glomeruli, but it does not necessarily result in lateral inhibition of neighboring modules.

The overall effect of inhibitory and excitatory inputs depends on the targets of these inputs. The proportion of PG and ET cells targeted by PG axons derived from neighboring modules and the synaptic efficiency of these synapses are still unknown, therefore the net effect of feed-forward inhibition is hard to predict. We can speculate that PG cells are more frequently targeted by GABAergic inputs than ET cells (7 of 19 PG cells (37%) and 1 of 5 ET cells (20 %) had monosynaptic IPSP). In this case monosynaptic feed-forward inhibition targeting PG cells in adjacent glomeruli can facilitate spread of excitation of their neuronal ensembles. At the same time, moderate excitatory input to ET cells of distant glomeruli can facilitate excitation of these modules, unless the strength of the input exceeds a certain threshold, when critical amount of activated PG cells will shut down the excitation. In other words, low level of activity in the central glomerulus can facilitate (a) excitation among adjacent ensembles via feed-forward inhibition of their inhibitory PG cells, and (b) in distant ensembles via low intensity excitatory inputs from SA-network. This helps to maintain background ("alert") level of activation in the system. However, strong excitatory input to a given glomerulus from another one will lead to its intrinsic feedback inhibition. In this case, the extensive SA-network can provide lateral inhibition in the majority of modules around the excited central module [center-surround inhibition, Aungst et al., 2003]. With an intermediate level of input signal to the central glomerulus (most relevant to a given odor) an interplay between the SA excitatory network and local PG cell-mediated feed-forward inhibition can bring some other modules up to threshold, thus increasing their sensitivity to their own sensory inputs and forming a specific intensity-dependent pattern of activated modules. It is likely, that center-surround inhibition is an extreme case in the operational range of the glomerular layer modular subsystem, providing suppression of glomerular map codes for all or most of odors that are significantly weaker than the strong dominating smell.

This is supported by data in a specially designed experiment in which all OB layers, except for the glomerular layer, were cut between the stimulated site and the site containing the apical tuft of a mitral cell [Aungst et al., 2003]. In that experiment, LLD in a mitral cell elicited by ONL stimulation was curtailed by a delayed strong stimulation in the GL from the other side of the cut. The GL stimulation alone evoked at about 6 ms latency a di- or polysynaptic IPSP, which was completely blocked by gabazine. This result indicates the presence of excitatory interglomerular connections that activate local GABAergic PG cells to

cause postsynaptic inhibition of mitral cells. When the paired ONL-GL stimulation was applied in the presence of gabazine, LLD was no longer suppressed.

18. SPONTANEOUS INTERGLOMERULAR INTERACTIONS

The occasional positive cross-correlation of sGLFPs in remote glomeruli corroborates the assumption that during background activity cross-talk between glomerular populations involves exchange of excitatory signals that do not lead to a significant lateral inhibition. Such level of activity is probably analogous to a very weak (subthreshold) input from the olfactory epithelium. The significant positive peaks in some cross-correlograms indicate simultaneous or slightly delayed occurrence of population events in distant glomeruli (Figure 14 *K*-*O*).

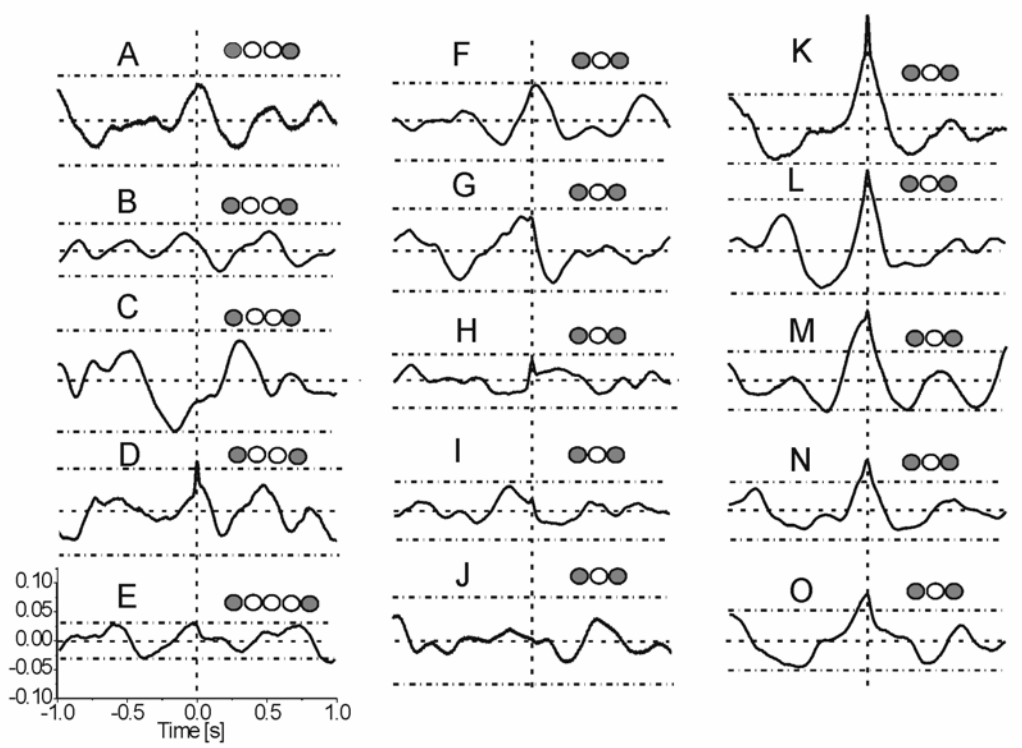

Figure 14. Cross-correlation of spontaneous field potentials recorded in pairs of remote glomeruli. Cross-correlation functions (CCFs) in the left and middle columns indicate the absence of significant cross-correlation. CCFs in the right column show significant cross-correlation around zero time lag. Horizontal dashed lines in each plot designate confidence levels ($\pm \Delta$, $p<0.01$) above and below the zero level (CCF=0). Vertical dashed lines indicate zero time lag ($\tau=0$). Hollow circles designate glomeruli separating recording sites (filled circles). Sharp peaks at $\tau=0$ overriding slow waves in some CCFs (*D*, *H*, *I*, *K*, *M*) may indicate a spontaneous synchronous common synaptic input (e.g. from the ON). Epoch of analysis for each CCF was 200 s.

Lateral inhibition, if present, would result in a trough around the central point indicating negative cross-correlation. Finally, it becomes clear that the synaptic arrangement among

modules in the glomerular map of the olfactory bulb is not as simple as it was originally thought. The interplay of different signs of synaptic transmission which are intensity- and distance-dependent, the temporal shifts and delays in developing modular patterns, and the specific patterns of non-uniformly activated compartments within glomeruli may create a dynamic spatial-temporal image of the odor's identity. Such dynamic odor image on the MOB odor map should operate with a spatially and temporally structured activity of olfactory receptor neurons, because diverse glomerulus- and odorant-dependent temporal dynamics have been shown even at this initial input stage [Spors et al., 2006]. Temporally organized interactions among glomerular modules may further elaborate the initial temporally structured dynamic of primary sensory inputs. Interactions among modules can also be relevant to formation of molecular-feature glomerular clusters, which are located at stereotypical positions in the OB and might be part of the neural representation of basic odor quality [Mori et al., 2006]. Each fractionated component of an odor mixture has been shown to activate only one or few glomeruli. Therefore a glomerular pattern in response to a complex stimulus is the sum of the responses to its individual components, and activation of an individual glomerulus independently signals the presence of a specific component [Lin de et al., 2006]. Inter-glomerular links should be available and readily used to re-create the odor entity from its components at the first stage of odor processing in the CNS. Excessive interglomerular connections are the substrate for constructing a multitude of glomerular patterns.

19. GLOMERULAR LAYER AS A SPECIALIZED SUB-SYSTEM OF THE MOB

Principle of modular organization is not unique to the olfactory bulb; for example, columnar organization has been found in the mammalian neocortex [Mountcastle, 1957], and such structural feature was shown to play a role in the organization of functional neocortical ensembles subserving different modalities [Chebkasov, 2000; Goldschmidt et al., 2004; Vnek et al., 1999; for review: Mountcastle, 1997; Diamond et al., 2003; Kaas., 1993). However, except for the barrels in the rodent somato-sensory cortex [Feldman and Peters, 1974; Weller, 1972; Woolsey and Van der Loos, 1970], there are no distinctive anatomical borderlines among partially overlapping functional ensembles of the neocortex. In this respect, the olfactory glomerulus represents the most distinctive multicellular module with all associated neurons functionally bound by their dendritic tufts in a spatially localized spheroid. However, since a glomerular unit defines a population of functionally related neurons that extend across multiple layers [Chen and Shepherd, 2005; Willhite et al., 2006], not all its neurons are localized in precisely predictable points; for example, the somata of M/T cells can be located at various distances from their glomerulus and their lateral/secondary dendrites span over 1 mm distance in the EPL. Thus, although the upper (glomerular) part of the module can be unequivocally determined and is spatially separated from others, the deeper part containing M/T cells is remote from the glomerulus and spatially dispersed (Figure 15, green cells). Furthermore, spatial separation of the tuft and lateral dendrites of mitral cells has been shown to be critical for correct performance of these output cells, otherwise excitatory input and electrical coupling in tufts would interfere with lateral inhibition by granule cells [Migliore et al., 2005].

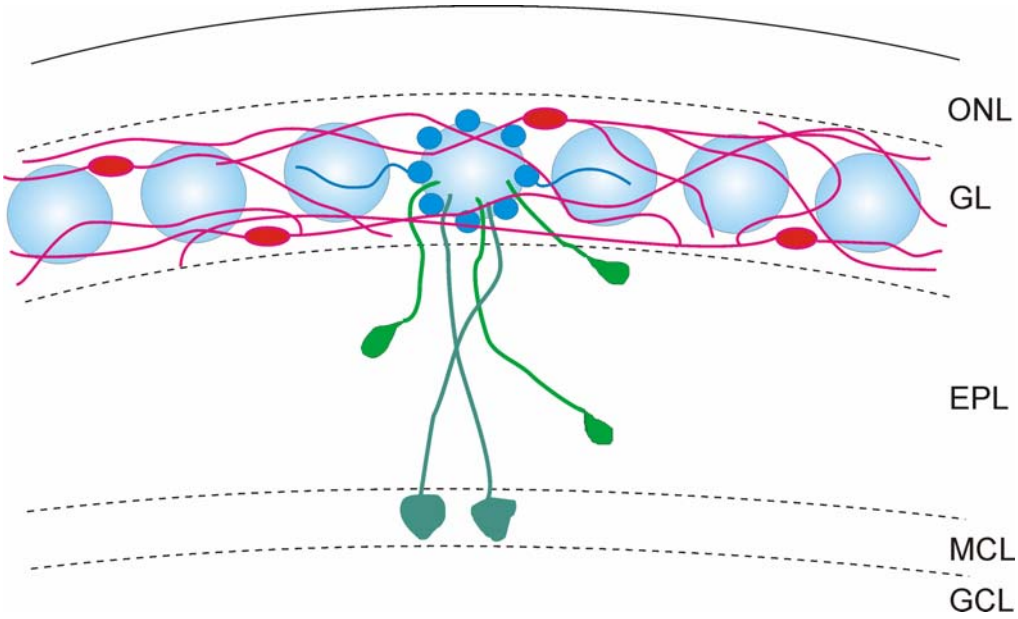

Figure 15. Diagram of the glomerular layer modular subsystem. One depicted complete module includes one glomerulus and associated with it JG (blue) and M/T (green) cells. Short axons of PG cells provide feedforward inhibition in adjacent glomeruli. Long axons of SA cells (red) provide excitatory interactions among modules in a broad area. Granule cells do not belong to individual modules, therefore they are not included to the modular subsystem. Lateral dendrites of mitral cells and secondary dendrites of tufted cells propagating in the EPL, as well as all intraglomerular ramifications, are omitted.

Deeper M/T cell ensembles that are associated with the same MOB modules are anatomically similar to cortical modules as they are embedded into each other, although they do not communicate directly due to lack of synaptic contacts in the EPL. Mutual penetration of structural units implies higher probability of interactions among them. Indeed, there is growing evidence that olfactory modules are not functionally isolated because they are capable of coordinating their activity via mitral-to-granule-to-mitral cell interactions (lateral inhibition) in the EPL [Freidman and Strowbridge, 2003; Lagier et al., 2004; Schoppa et al., 1998], via mitral-to-mitral cell interactions (glutamate spillover onto NMDA receptors in the EPL) [Friedman and Strowbridge, 2000], and via the network of SA cells in the GL (center-surround inhibition) [Aungst et al, 2003]. Due to random orientation of the lateral/secondary dendrites of M/T cells and random targeting of a few M/T cells by the same granule cell, cross-talk in the EPL is not module-selective and is thought to increase signal-to-noise ratio by lateral inhibition [Shepherd and Brayton, 1979]. Surprisingly, interactions among modules within the GL seem to be more specific, although the upper parts of the modules are spatially isolated.

It has been recently recognized that the mammalian olfactory system is not uniformly organized but consists of several subsystems, each of which probably serves distinct functions [Breer et al., 2006]. Based on the above and previous results [Aungst et al., 2003; Hayar et al., 2004a, 2004b], we hypothesize that the GL represents a subsystem of glomerular modules interconnected via inhibitory PG cells at short distances (1-3 glomeruli) and via excitatory SA cells at relatively longer distance (up to 20 glomeruli) (Figure 15). This glomerular layer

subsystem begins odor analysis a few milliseconds earlier than the onset of output signals (evoked spikes) in M/T cells. Because of its unique structural-functional characteristics, this subsystem may serve as a band-pass odor intensity discriminator (Figure 16).

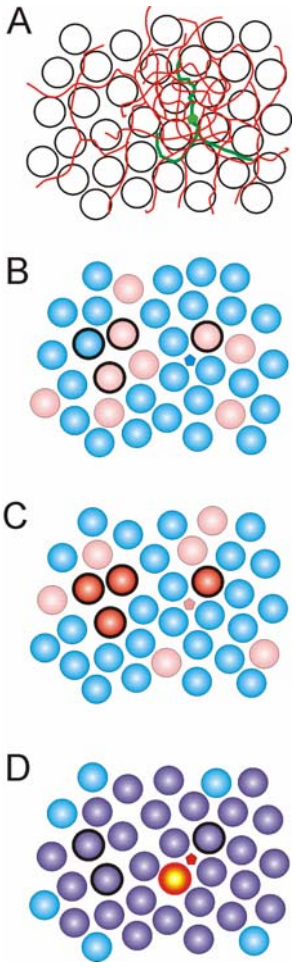

Figure 16. Three operational modes of the hypothesized odor intensity serve as a band-pass discriminator. *A* – glomerular map with a dormant SA cell (green pentagon); red lines represent SA cell axonal arborization. *B* – instant background pattern of the GL activity; blue balls designate dormant glomeruli, pink balls designate sGLFP-generating glomeruli. *C* – moderate sensory input reveals a steady odor-related pattern of activated modules (red) from arbitrary blinking sGLFP patterns (pink); SA cell (now light red) delivers moderate excitatory inputs to its targets, creating spatial-temporal image of the odor. *D* – strong sensory input causes strong excitation of the corresponding glomerulus (yellow flashed red ball) and the adjacent SA cells (now bright red); SA cells deliver strong excitatory input to surrounding modules, which is now sufficient to trigger recurrent inhibition in each of them and make them temporarily insensitive to any other inputs (purple). In this state the system is unable to distinguish fine aromas or odor blends, and senses only the dominant smell.

In this case, sGLFPs continuously create spatially distributed "white noise" in the glomerular map preventing detection of weak odors (Figure 16 *B*). This relatively low level of discrimination might be necessary to ignore occasional odor molecules and to keep the system alert for significant signals. The high level of discrimination may be formed by lateral

inhibition. In this case, high odor intensity can strongly excite a corresponding glomerulus and then result in widespread lateral interglomerular inhibition mediated by SA cells, a mechanism that eliminates perception of all other odors but the prevailing one (Figure 16 *D*). At intermediate odor intensities, different patterns of activated glomeruli can emerge from noisy sGLFP background without being suppressed by lateral inhibition (Figure 16 *C*). This allows discrimination of fine aromas or odor blends. Even though the activity of neurons in the glomerular module is tightly correlated, there might be fine spatial and temporal relations of different neuronal elements within the module. The fact that occurrence of output signals is delayed (~ 50-170 ms) relative to intraglomerular activation and that interglomerular communication occurs in a shorter time window (tens of ms), indicates that output neurons are recruited to information processing after an initial processing within the glomerular layer has started. This also supports the hypothesis that the glomerular layer is critical for initial odor analysis and it operates as the first-line subsystem for the spatial-temporal encoding of complex sensory signals.

CONCLUSION

Temporal firing patterns, including neuronal synchronization and network oscillations, are thought to be important in sensory information processing including odor coding. Odor-evoked activity in the mammalian olfactory bulb contains both fast and slow network oscillatory components. Investigative sniffing and concomitant olfactory network oscillations occur in the slower theta frequency range. Patterned sensory input resulting from active "theta sniffing" is thought to establish rhythmical activity patterns in the olfactory bulb that enhance odor processing. ET cells are located at the first site of synaptic processing in the olfactory system and they spontaneously generate rhythmic spike bursts that are highly correlated among ET cells of the same glomerulus. ET cell spike bursts are readily entrained by patterned sensory input at “sniffing” frequencies. Thus, the ensemble of ET cells of each glomerulus might function as a network oscillator whose rhythm is entrained by patterned sensory input. The synchronous activity of the ET cell ensemble of a given glomerulus could provide synchronous excitatory burst onto mitral cells, the output neurons of the olfactory bulb. Indeed, mitral cells associated with the same glomerulus exhibit synchronous long-lasting depolarizations that are thought to be caused by a sustained recurrent excitatory synaptic activity of glomerular origin. Because the temporal summation of EPSPs produced by coincident presynaptic bursts increases the likelihood of spike initiation in postsynaptic neurons, synchronization of odor-evoked glomerular output (i.e., mitral cell spikes) by the ET cell network could ensure that glomerular output is faithfully transferred to higher order olfactory structures. Modular organization of different neuron types into structural and functional unit allows for reliable signal transfer regardless of probabilistic activation of individual cells. Interactions among modules create a higher level of functional hierarchy providing initial odor analysis right on the front line of the information processing, elaborating spatial-temporal coding, and probably modulating sensation of the odor in successive sniffing cycles.

ACKNOWLEDGMENTS

We acknowledge support from PHS grants DC06356, and DC07123, RR020146.

REFERENCES

Adrian, E.D. (1950). The electrical activity of the olfactory bulb. *Electroenceph. Clin. Neurophysiol., 2 ,* 377-388.

Alonso, J.M., Usrey, W.M., and Reid, R.C. (1996). Precisely correlated firing in cells of the lateral geniculate nucleus. *Nature, 383*, 815-819.

Alreja, M., and Aghajanian, G.K. (1995). Use of the whole-cell patch-clamp method in studies on the role of cAMP in regulating the spontaneous firing of locus coeruleus neurons. *J. Neurosci. Methods, 59*, 67-75.

Antal, M., Eyre, M., Finklea B., and Nusser Z. (2006). External tufted cells in the main olfactory bulb from two distinct subpopulations. *European J. Neurosci.*, *24*, 1124-1136.

Aroniadou-Anderjaska, V., Ennis, M., and Shipley, M.T. (1997). Glomerular synaptic responses to olfactory nerve input in rat olfactory bulb slices. *Neurosci., 79*, 425-434.

Aroniadou-Anderjaska, V., Ennis, M., and Shipley, M.T. (1999). Dendrodendritic recurrent excitation in mitral cells of the rat olfactory bulb. *J. Neurophysiol., 82*, 489-494.

Aroniadou-Anderjaska, V., Zhou, F.M., Priest, C.A., Ennis, M., and Shipley, M.T. (2000). Tonic and synaptically evoked presynaptic inhibition of sensory input to the rat olfactory bulb via GABA(B) heteroreceptors. *J. Neurophysiol., 84*, 1194-1203.

Aungst, J.L., Heyward, P.M., Puche, A.C., Karnup, S.V., Hayar, A., Szabo, G., and Shipley, M.T. (2003). Center-surround inhibition among olfactory bulb glomeruli. *Nature, 426*, 623-629.

Azouz, R., Jensen, M.S., and Yaari, Y. (1996). Ionic basis of spike after-depolarization and burst generation in adult rat hippocampal CA1 pyramidal cells. *J. Physiol., 492*, 211-223.

Bailey, M.S., and Shipley, M.T. (1993). Astrocyte subtypes in the rat olfactory bulb: morphological heterogeneity and differential laminar distribution. *J. Comp. Neurol., 328*, 501-526.

Baker, H., Margolis, F.L. (2002). Mechanisms of differentiation and migration of the olfactory progenitors: an overview. *Chem. Senses, 27(6)*, 567.

Banay-Schwartz, M., Lajtha, A., and Palkovits, M. (1989a). Changes with aging in the levels of amino acids in rat CNS structural elements: I. glutamate and related amino acids. *Neurochem. Res., 14*, 555–562.

Banay-Schwartz, M., Lajtha, A., and Palkovits, M. (1989b). Changes with aging in the levels of amino acids in rat CNS structural elements: II. taurine and small neutral amino acids. *Neurochem. Res., 14*, 563–570.

Bardoni, R., Magherini, P.C., and Belluzzi, O. (1995). Sodium current in periglomerular cells of frog olfactory bulb *in vitro*. *Brain. Res., 703*, 19-25.

Bardoni, R., Magherini, P.C., and Belluzzi, O. (1996). Excitatory synapses in the glomerular triad of frog olfactory bulb *in vitro*. *Neuro. Report, 7*, 1851-1855.

Belluscio, L., Katz, L.C. (2001). Symmetry, stereotypy, and topography of odorant representations in mouse olfactory bulbs. *J. Neurosci., 21*, 2113-2122.

Belluzzi, O., Benedusi, M., Ackman, J., and LoTurco, J. (2003). Electrophysiological identification of new neurons in the olfactory bulb. *J. Neurosci., 23*, 10411-10418.

Berkowicz, D.A., and Trombley, P.Q. (2000). Dopaminergic modulation at the olfactory nerve synapse. *Brain Res., 855*, 90-99.

Biffo, S., Grillo, M., and Margolis, F.L. (1990). Cellular localization of carnosine-like and anserine-like immunoreactivities in rodent and avian central nervous system. *Neurosci., 35*, 637-651.

Björklund, H., and Lindvall, O. (1984). Dopamine-containing systems in the CNS. In: A. Björklund and T. Hokfelt (Eds.) *Handbook of Neuroanatomy* (pp. 55-122). Amsterdam, ST: Elsevier.

Blanes, T. (1898). Sobre algunos puntos dudosos de la estructura del bulbo olfactorio. *Revista. Trimestral. microgafica*, 3, 99-127.

Bokil, H., Laaris, N., Ennis, M., and Keller, A. (2001). Ephaptic interactions in the mammalian olfactory system. *J. Neurosci.*, 21, RC173.

Bonino, M., Cantino, D., and Sassoe-Pognetto, M. (1999). Cellular and subcellular localization of gamma-aminobutyric acid receptors in the rat olfactory bulb. *Neurosci. Lett., 274*, 195-198.

Bowery, N.G., Hudson, A.L., and Price, G.W. (1987). $GABA_A$ and $GABA_B$ receptor site distribution in the rat central nervous system. *Neurosci., 20*, 365-383.

Breer, H. (2003). Olfactory receptors: molecular basis for recognition and discrimination of odors. *Anal. Bioanal. Chem., 377*, 427-433.

Breer, H., Fleischer, J., and Strotmann, J. (2006). The sense of smell: multiple olfactory subsystems. *Cell Mol. Life Sci.*, 2006 May 29; [E-pub ahead of print]

Brumberg, J.C., Nowak, L.G., and McCormick, D.A. (2000). Ionic mechanisms underlying repetitive high-frequency burst firing in supragranular cortical neurons. *J. Neurosci.*, 20, 4829-4843.

Cajal, S.R.y. (1911a). Olfactory apparatus: olfactory mucosa and olfactory bulb or first-order olfactory center, In: *Histology of the Nervous System*, Vol. II. (Translated by N. Swanson and L. Swanson (1995)), (pp. 532-554). New York, ST: Oxford Univ. Press.

Cajal, R.S.y. (1911b). *Histologie du Systeme Nerveux de l'Hommes et des Vertebres*. Paris: ST: Maloine.

Cang, J., and Isaacson, J.S. (2003). *In vivo* whole-cell recording of odor-evoked synaptic transmission in the rat olfactory bulb. *J. Neurosci., 23*, 4108-4116.

Carlson, G.C., Shipley, M.T., and Keller, A. (2000). Long-lasting depolarizations in mitral cells of the rat olfactory bulb. *J. Neurosci., 20*, 2011-2021.

Chao, T.I., Kasa, P., and Wolff, R. (1997) Distribution of astroglia in glomeruli of the rat main olfactory bulb: exclusion from the sensory subcompartment of neuropil. *J. Comp. Neurol., 338,* 191-210.

Charpak, S., Mertz, J., Beaurepaire, E., Moreaux, L., and Delaney, K. (2001). Odor-evoked calcium signals in dendrites of rat mitral cells. *Proc. Natl. Acad. Sci., 98,* 1230-1234.

Chebkasov, S.A. (2000). Tangential segregation of simple and complex cells in the visual cortex and their connections. A universal neocortical module. *Neurosci. Behav. Physiol.*, *30*, 89-96.

Chen, W.R. and Shepherd, G.M. (1997). Membrane and synaptic properties of mitral cells in slices of rat olfactory bulb. *Brain Res., 745*, 189-196.

Chen, W.R. and Shepherd, G.M. (2005). The olfactory glomerulus: a cortical module with specific functions. *J. Neurocytology, 34,* 353-360.

Christie, J.M. and Westbrook, G.L. (2006). Lateral excitation within the olfactory bulb. *J. Neurosci., 26*, 2269-2277.

Christie, J.M., Bark, C., Hormuzdi, S.G., Helbig, I., Monyer, H. and Westbrook, G.L. (2005). Connexin36 mediates spike synchrony in olfactory bulb glomeruli. *Neuron., 46*, 761-772.

Chu, D.C.M., Albin, R.L., Young, A.B. and Penney, J.B. (1990). Distribution and kinetics of GABAB binding sites in rat central nervous system: a quantitative autoradiographic study. *Neurosci., 34*, 341-357.

Cinelli, A.R., Hamilton, K.A., and Kauer, J.S. (1995). Salamander olfactory bulb neuronal activity observed by video rate, voltage-sensitive dye imaging. III. Spatial and temporal properties of responses evoked by odorant stimulation. *J. Neurophysiol., 73,* 2053-2071.

Collins, G.G. (1974). The rates of synthesis, uptake and disappearance of [14C]-taurine in eight areas of the rat central nervous system. *Brain Res., 76*, 447–459.

Coronas, V., Srivastava, L.K., Liang, J.J., Jourdan, F. and Moyse, E. (1997). Identification and localization of dopamine receptor subtypes in rat olfactory mucosa and bulb: a combined in situ hybridization and ligand binding radioautographic approach. *J. Chem. Neuroanat., 12*, 243-257.

Cornwall, J. and Phyllipson, O.T. (1988). Quantitative analysis of axonal branching using a retrograde transport of fluorescent latex microspheres. *J. Neurosci. Methods, 24,*1-9.

Coskun, V., and Luskin, M.B. (2002). Intrinsic and extrinsic regulation of the proliferation and differentiation of cells in the rodent rostral migratory stream. *J. Neurosci. Res., 69(6),* 795-802.

Davis, B.J. and Macrides, F. (1983). Tyrosine hydroxylase immunoreactive neurons and fibers in the olfactory system of the hamster. *J. Comp. Neurol., 214*, 427-440.

De Saint Jan, D. and Westbrook, G.L. (2005). Detecting activity in olfactory bulb glomeruli with astrocyte recording. *J. Neurosci., 25*, 2917-2924.

Debarbieux, F., Audinat, E. and Charpak S. (2003). Action potential propagation in dendrites of rat mitral cells *in vivo*. *J. Neurosci., 23*, 5553-5560.

Diamond, M.E., Petersen, R.S., Harris, J.A., and Panzeri, S. (2003). Investigations into the organization of information in sensory cortex. *J. Physiol. Paris*, *97(4-6)*, 529-36.

Didier, A., Ottersen, O.P. and Storm-Mathisen, J. (1994). Differential subcellular distribution of glutamate and taurine in primary olfactory neurons. *NeuroReport, 6*, 145–148.

DiFrancesco, D. (1993). Pacemaker mechanisms in cardiac tissue. *Annu. Rev. Physiol., 55*, 455-472.

Doty, R.L. and Risser, J.M. (1989). Influence of the D-2 dopamine receptor agonist quinpirole on the odor detection performance of rats before and after spiperone administration. *Psychopharmacol., 98*, 310-315.

Doucette, R. (1989). Development of the nerve fiber layer in the olfactory bulb of mouse embryos. *J. Comp. Neurol., 285*, 514-527.

Duchamp-Viret, P., Chaput, M.A. and Duchamp, A. (1999). Odor response properties of rat olfactory receptor neurons. *Science, 284*, 2171-2174.

Eeckman, F.H. and Freeman, W.J. (1990). Correlations between unit firing and EEG in the rat olfactory system. *Brain Res., 528*, 238-244.

Ekstrand J.J., Domroese M.E., Johnson D.M., Feig S.L. Knodel S.M., Behan M and Haberly L.B. (2001). A new subdivision of anterior piriform cortex and associated deep nucleus with novel features of interest for olfaction and epilepsy. *J. Comp. Neurol., 434,* 289-307.

Ennis, M., Zhou, F.M., Ciombor, K.J., Aroniadou-Anderjaska, V., Hayar, A., Borrelli, E., Zimmer, L.A., Margolis, F. and Shipley, M.T. (2001). Dopamine D2 receptor-mediated presynaptic inhibition of olfactory nerve terminals. *J. Neurophysiol., 86*, 2986-2997.

Ennis, M., Zimmer, L.A. and Shipley, M.T. (1996). Olfactory nerve stimulation activates rat mitral cells via NMDA and non- NMDA receptors *in vitro*. *NeuroReport, 7*, 989-992.

Ennis, M., Zhu. M. and Hayar, A. (2006). Olfactory nerve-evoked, metabotropic glutamate receptor-mediated synaptic responses in rat olfactory bulb mitral cells. *J. Neurophysiol., 95*, 2233-2241.

Ferriero, D. and Margolis, F.L. (1975). Denervation in the primary olfactory pathway of mice. II. Effects on carnosine and other amine compounds. *Brain Research, 94*, 75-86.

Friedman, D. and Strowbridge, B.W. (2000). Functional role of NMDA autoreceptors in olfactory mitral cells. *J Neurophysiol, 84*, 39-50.

Friedrich, R.W. (2002). Real time odor representations. *Trends Neurosci., 25*, 487-489.

Fukushima, N., Yokouchi, K., Kawagishi, K., and Moriizumi, T. (2002). Differential neurogenesis and gliogenesis by local and migrating neural stem cells in the olfactory bulb. *Neurosci. Res., 44(4),* 467-73.

Gall, C., Seroogy, K.B. and Brecha, N. (1986). Distribution of VIP- and NPY-like immunoreactivities in rat main olfactory bulb. *Brain Res., 374*, 389-394.

Gelperin, A. (2006). Olfactory computations and network oscillation. *J. Neurosci., 26*, 1663-1668.

Getchell, T.V. and Shepherd, G.M. (1975). Synaptic actions on mitral and tufted cells elicited by olfactory nerve volleys in the rabbit. *J Physiol, 251*, 497-522.

Golgi, C. (1875). Sulla Fina Structrura del Bulbi Olfattori. *Rev. Sper. Feniatr., 1*, (pp. 405-425). Rome, ST: Reggio Emilla.

Goldschmidt, J., Zuschratter, W., and Scheich, H. (2004). High-resolution mapping of neuronal activity by thallium autometallography. *Neuroimage, 23*, 638-647.

Halász, N., Hokfelt, T., Norman, A.W. and Goldstein, M. (1985). Tyrosine hydroxylase and 28K-vitamin D-dependent calcium binding protein are localized in different subpopulations of periglomerular cells of the rat olfactory bulb. *Neurosci. Lett., 61*, 103-107.

Halász, N., Ljungdahl, A., Hokfelt, T., Johansson, O., Goldstein, M., Park, D. and Biberfeld, P., (1977). Transmitter histochemistry of the rat olfactory bulb. I. Immunohistochemical localization of monoamine synthesizing enzymes. Support for intrabulbar, peri-glomerular dopamine neurons. *Brain Res., 126*, 455-474.

Hayar, A., Karnup, S., Shipley, M.T. and Ennis, M. (2004a). Olfactory bulb glomeruli: external tufted cells intrinsically burst at theta frequency and are entrained by patterned olfactory input. *J. Neurosci., 24*, 1190-1199.

Hayar, A., Karnup, S., Ennis, M. and Shipley, M.T. (2004b). External tufted cells: a major excitatory element that coordinates glomerular activity. *J. Neurosci., 24*, 6676-6685.

Hayar, A., Shipley, M.T. and Ennis, M. (2005). Olfactory bulb external tufted cells are synchronized by multiple intraglomerular mechanisms. *J. Neurosci., 25*, 8197-8208.

Haberly L.B. and Price J.L. (1977). The axonal projection patterns of the mitral and tufted cells of the olfactory bulb in the rat. *Brain Res., 129*, 152-157.

Hsia, A.Y., Vincent, J.D. and Lledo, P.M. (1999). Dopamine depresses synaptic inputs into the olfactory bulb. *J. Neurophysiol., 82*, 1082–1085.

Isaacson, J.S. (1999). Glutamate spillover mediates excitatory transmission in the rat olfactory bulb. *Neuron, 23*, 377-384.

Isaacson, J.S. and Strowbridge, B.W. (1998). Olfactory reciprocal synapses: dendritic signaling in the CNS. *Neuron, 20*, 749-761.

Jahr, C.E. and Nicoll, R.A. (1981). Primary afferent depolarization in the in vitro frog olfactory bulb. *J. Physiol. (Lond), 318*, 375-384.

Johnson, B.A., and Leon, M. (2000a). Modular representations of odorants in the glomerular layer of the rat olfactory bulb and the effects of stimulus concentration. *J. Comp. Neurol., 422*, 496-509.

Johnson, B.A., and Leon, M. (2000b). Odorant molecular length: one aspect of the olfactory code. *J. Comp. Neurol., 426*, 330-338.

Jourdan, F., Duveau, A., Astic, L., and Holley, A. (1980). Spatial distribution of [14C]2-deoxyglucose uptake in the olfactory bulbs of rats stimulated with two different odours. *Brain Res., 188*, 139-154.

Kaas, J.H. (1993). Evolution of multiple areas and modules within neocortex. *Perspect. Dev. Neurobiol., 1(2)*, 101-107.

Kamisaki, Y., Wada, K., Nakamoto, K. and Itoh, T. (1996). Effects of taurine on GABA release from synaptosomes of rat olfactory bulb. *Amino Acids, 10*, 49–57.

Karnup, S.V., Hayar, A., Shipley, M.T., and Kurnikova, M.G. (2006). Spontaneous Field Potentials in the Glomeruli of the Olfactory Bulb: the Leading Role of Juxtaglomerular Cells. *Neurophysiol.*, [e-pub. ahead of print].

Karnup, S., and Stelzer, A. (1999). Temporal overlap of excitatory and inhibitory afferent input in CA1 pyramidal cells. *J. Physiology, 516*, 485-504.

Kasowski, H.J., Kim, H. and Greer, C.A. (1999). Compartmental organization of the olfactory bulb glomerulus. *J. Comp. Neurol., 407*, 261-274.

Karwoski, C.J., Lu, H.K., and Newman, E.A. (1989). Spatial buffering of light-evoked potassium increases by retinal Müller (glial) cells. *Science, 244*, 578-580.

Kauer, J.S. (1998). Olfactory processing: a time and place for everything. *Curr. Biol., 8*, R282-R283.

Kay, L.M. (2003). A challenge to chaotic intinerancy from brain dynamics. *Chaos, 13*, 1057-1066.

Kay, L.M. (2005). Theta oscillations and sensorimotor performance. *Proc. Natl. Acad. Sci. U S A, 102*, 3863-3868.

Kay, L.M. and Laurent, G. (1999). Odor- and context-dependent modulation of mitral cell activity in behaving rats. *Nat. Neurosci., 2*, 1003-1009.

Keller, A., Yagodin, S., Aroniadou-Anderjaska, V., Zimmer, L.A., Ennis, M., Sheppard, N.F., Jr. and Shipley, M.T. (1998). Functional organization of rat olfactory bulb glomeruli revealed by optical imaging. *J. Neurosci., 18*, 2602-2612.

Kepecs, A., Uchida, N. and Mainen, Z.F. (2006). The sniff as a unit of olfactory processing. *Chem. Senses, 31*, 167-179.

Khayari, A., Math, F., and Davrainville, J.L. (1988). Electrical stimulation of primary olfactory nerve induces two types of variations in the extracellular potassium activity within the glomerulus of the rat olfactory bulb in vivo. *Brain Res., 457*, 188-191.

Kofuji, P., and Newman, E.A. (2004). Potassium buffering in the central nervous system. *Neuroscience, 129*, 1045-1056.

Komisaruk, B.R. (1970). Synchrony between limbic system theta activity and rhythmical behavior in rats. *J. Comp. Physiol. Psychol., 70*, 482-492.

Konig, P., Engel, A.K. and Singer, W. (1996). Integrator or coincidence detector? The role of the cortical neuron revisited. *Trends Neurosc., 19*, 130-137.

Kosaka, K., Hama, K., Nagatsu, I., Wu, J.Y. and Kosaka, T. (1988). Possible coexistence of amino acid (gamma-aminobutyric acid), amine (dopamine) and peptide (substance P); neurons containing immunoreactivities for glutamic acid decarboxylase, tyrosine hydroxylase and substance P in the hamster main olfactory bulb. *Exp. Brain Res., 71*, 633-642.

Kosaka, K., Hama, K., Nagatsu, I., Wu, J.Y., Ottersen, O.P., Storm-Mathisen, J. and Kosaka, T. (1987a). Postnatal development of neurons containing both catecholaminergic and GABAergic traits in the rat main olfactory bulb. *Brain Res. ,403*, 355-360.

Kosaka, K., Toida, K., Aika, Y. and Kosaka, T. (1998). How simple is the organization of the olfactory glomerulus?: the heterogeneity of so-called periglomerular cells. *Neurosci Res., 30*, 101-110.

Kosaka, K., Toida, K., Margolis, F.L. and Kosaka, T. (1997). Chemically defined neuron groups and their subpopulations in the glomerular layer of the rat main olfactory bulb--II. Prominent differences in the intraglomerular dendritic arborization and their relationship to olfactory nerve terminals. *Neurosci., 76*, 775-786.

Kosaka, T. and Kosaka, K. (2003). Neuronal gap junctions in the rat main olfactory bulb, with special reference to intraglomerular gap junction. *Neurosci. Res., 45*, 189-209.

Kosaka, T. and Kosaka, K. (2004). Neuronal gap junctions between intraglomerular mitral/tufted cell dendrites in the mouse main olfactory bulb. *Neurosci. Res., 49*, 373-378.

Kosaka K and Kosaka T (2005). Synaptic organization of the glomerulus in the main olfactory bulb: Compartments of the glomerulus and heterogeneity of the periglomerular cells. *Anatomical Science International, 80*, 80-90.

Kosaka, T., Hataguchi, Y., Hama, K., Nagatsu, I. and Wu, J.Y. (1985). Coexistence of immunoreactivities for glutamate decarboxylase and tyrosine hydroxylase in some neurons in the periglomerular region of the rat main olfactory bulb: possible coexistence of gamma-aminobutyric acid (GABA) and dopamine. *Brain Res., 343*, 166-171.

Kosaka, T., Kosaka, K., Hama, K., Wu, J.-Y. and Nagatsy, I. (1987b). Differential effect of functional olfactory deprivation on the GABAergic and catecholaminergic traits in the rat main olfactory bulb. *Brain Res., 413*, 197-203.

Kosaka, T., Kosaka, K., Hataguchi, Y., Nagatsu, I., Wu, J.Y., Ottersen, O.P., Storm-Mathisen, J. and Hama, K. (1987c). Catecholaminergic neurons containing GABA-like and/or glutamic acid decarboxylase-like immunoreactivities in various brain regions of the rat. *Exp. Brain Res., 66*, 191-210.

Kosaka, T., Kosaka, K., Heizmann, C.W., Nagatsu, I., Wu, J.Y., Yanaihara, N. and Hama, K. (1987d). An aspect of the organization of the GABAergic system in the rat main olfactory bulb: laminar distribution of immunohistochemically defined subpopulations of GABAergic neurons. *Brain Res., 411*, 373-378.

Koster, N.L., Norman, A.B., Richtand, N.M., Nickell, W.T., Puche, A.C., Pixley, S.K. and Shipley, M.T. (1999). Olfactory receptor neurons express D2 dopamine receptors. *J. Comp. Neurol., 411*, 666-673.

Kratskin, I. and Belluzzi, O. (2003). Anatomy and neurochemistry of the olfactory bulb. In R.L. Doty (Ed.), *Handbook of Olfaction and Gustation* (2nd edition, pp. 139-164). New York, ST: Marcel Dekker,.

Kratskin, I. and Belluzzi, O. (2002). Immunohistochemical localization of the taurine-synthesizing enzyme in the rat olfactory bulb. *Chem. Senses, 27*, 46.

Kratskin, I.L., Rio, J.P., Kenigfest, N.B., Doty, R.L. and Repérant, J. (2000). A light and electron microscopic study of taurine-like immunoreactivity in the main olfactory bulb of frogs. *J. Chem. Neuroanat., 18*, 87–101.

Lagier, S., Carleton, A. and Lledo, P.M. (2004). Interplay between local GABAergic interneurons and relay neurons generates gamma oscillations in the rat olfactory bulb. *J. Neurosci., 24*, 4382-4392.

Laurent, G., Stopfer, M., Friedrich, R.W., Rabinovich, M.I., Volkovskii, A., and Abarbanel, H.D. (2001). Odor encoding as an active, dynamical process: experiments, computation, and theory. *Annu. Rev. Neurosci., 24*,263-297.

Laurent, G. (2002). Olfactory network dynamics and the coding of multidimensional signals. *Nat. Rev. Neurosci., 3*, 884-895.

Levey, A.I., Hersch, S.M., Rye, D.B., Sunahara, R.K., Niznik, H.B., Kitt, C.A., Price, D.L., Maggio, R., Brann, M.R. and Ciliax, B.J. (1993). Localization of D1 and D2 dopamine receptors in brain with subtype-specific antibodies. *Proc. Natl. Acad. Sci. USA, 90*, 8861–8865.

Lin de, Y., Shea, S.D., and Katz,L.C. (2006). Representation of natural stimuli in the rodent main olfactory bulb. *Neuron, 50(6)*, 937-49.

Linster, C., and Cleland, T.A.. (2001). How spike synchronization among olfactory neurons can contribute to sensory discrimination. *J. Comput. Neurosci., 10*, 187-193.

Lisman, J.E. (1997). Bursts as a unit of neural information: making unreliable synapses reliable. *Trends Neurosci., 20*, 38-43.

Liu, W.-L. and Shipley, M.T. (1994). Intrabulbar associational system in the rat olfactory bulb comprises cholecystokinin-containing tufted cells that synapse onto the dendrites of GABAergic granule cells. *J. Comp. Neurol., 346*, 541-558.

Lledo, P.M., Gheusi, G. and Vincent, J.D. (2005). Information processing in the mammalian olfactory system. *Physiol. Rev., 85*, 281-317.

Lowe, G. (2003). Electrical signaling in the olfactory bulb. *Curr. Opin. Neurobiol., 13*, 476-481.

Luo, M. and Katz, L. (2001). Response correlation maps of neurons in the mammalian olfactory bulb. *Neuron, 32*, 1165-1179.

Lüthi, A. and McCormick, D.A. (1998). H-current: properties of a neuronal and network pacemaker. *Neuron, 21*, 9-12.

Macrides, F., Eichenbaum, H.B. and Forbes, W.B. (1982). Temporal relationship between sniffing and the limbic Θ rhythm during odor discrimination and reversal learning. *J Neurosci., 2*, 1705-1717.

Macrides, F. and Chorover, S.L. (1972). Olfactory bulb units: activity correlated with inhalation cycles and odor quality. *Science, 175*, 84-87.

Macrides F. and Schneider S. P. (1982). Laminar Organization of Mitral and Tufted Cells in the Main Olfactory Bulb of the Adult Hamster. *J. Comp. Neurol. 208*, 419-430.

Mansour, A., Meador-Woodruff, J.H., Bunzow, J.R., Civelli, O., Akil, H. and Watson, S.J. (1990). Localization of dopamine D2 receptor mRNA and D1 and D2 receptor binding in

the rat brain and pituitary: an in situ hybridization-receptor autoradiographic analysis. *J Neurosci., 10*, 2587-2600.

Margolis, F.L. (1974). Carnosine in the primary olfactory pathway. *Science, 184*, 909–911.

Margolis, F.L. (1980). Carnosine: an olfactory neuropeptide. In: *The role of peptides in neuronal function* (eds. J.L. Barker and T.G.J. Smith), p. 545-572. Marcel Dekker, New York.

Margrie, T.W. and Schaefer, A.T. (2003). Theta oscillation coupled spike latencies yield computational vigour in a mammalian sensory system. *J. Physiol., 546*, 363-374.

McLean, J.H. and Shipley, M.T. (1988). Postmitotic, postmigrational expression of tyrosine hydroxylase in olfactory bulb dopaminergic neurons. *J. Neurosci., 8*, 3658-3669.

McQuiston, A.R. and Katz, L.C. (2001). Electrophysiology of interneurons in the glomerular layer of the rat olfactory bulb. *J. Neurophysiol., 86*, 1899-1907.

Migliore, M., Hines, M.L. and Shepherd, G.M. (2005). The role of distal dendritic gap junctions in synchronization of mitral cell axonal output. *J. Computational Neuroscience, 18*, 151-161.

Mombaerts, P., Wang, F., Dulac, C., Chao, S.K., Nemes, A., Mendelsohn, M., Edmondson, J. and Axel, R. (1996). Visualizing an olfactory sensory map. *Cell, 87*, 675-686.

Mori, K., Kishi, K. and Ojima, H. (1983). Distribution of dendrites of mitral, displaced mitral, tufted, and granule cells in the rabbit olfactory bulb. *J. Comp. Neurol., 219*, 339-355.

Mori, K., Takahashi, Y.K., Igarashi, K.M., and Yamaguchi, M. (2006). Maps of odorant molecular features in the Mammalian olfactory bulb. *Physiol. Rev., 86(2)*, 409-33.

Mountcastle, V.B. (1957). Modality and topographic properties of single neurons in cat's somatic sensory cortex. *J. Neurophysiol., 20*, 408-434.

Mountcastle, V.B. (1997). The columnar organization of the neocortex. *Brain, 120(Pt 4)*, 701-722.

Mugnaini, E., Oertel, W.H. and Wouterlood, F.F. (1984). Immunocytochemical localization of GABA neurons and dopamine neurons in the rat main and accessory olfactory bulbs. *Neurosci. Lett.,47*, 221-226.

Murphy, G.J., Darcy, D.P. and Isaacson, J.S. (2005). Intraglomerular inhibition: signaling mechanisms of an olfactory microcircuit. *Nat. Neurosci., 8*, 354-364.

Mutoh, H., Yuan, Q. and Knöpfel, T. (2005). Long-term depression at olfactory nerve synapses *J. Neurosci., 25*, 4252-4259.

Newman, E.A. (1993). Inward-rectifying potassium channels in retinal glial (Müller) cells. *J. Neurosci., 13*, 3333-3345.

Nickell, W.T., Norman, A.B., Wyatt, L.M. and Shipley, M.T. (1991). Olfactory bulb DA receptors may be located on terminals of the olfactory nerve. *NeuroReport, 2*, 9-12.

Nowycky, M.C., Halasz, N. and Shepherd, G.M. (1983). Evoked field potential analysis of dopaminergic mechanisms in the isolated turtle olfactory bulb. *Neurosci., 8*, 717–722.

Orona, E., Rainer, E.C. and Scott, J.W. (1984). Dendritic and axonal organization of mitral and tufted cells in the rat olfactory bulb. *J. Comp. Neurol., 226*, 346-356.

Palouzier-Paulignan, B., Duchamp-Viret, P., Hardy, A.B. and Duchamp, A. (2002). GABA(B) receptor-mediated inhibition of mitral/tufted cell activity in the rat olfactory bulb: a whole-cell patch-clamp study *in vitro*. *Neurosci., 111*, 241-250.

Pape, H.C. (1996). Queer current and pacemaker: the hyperpolarization-activated cation current in neurons. *Annu. Rev. Physiol., 58*, 299-327.

Pignatelli, A., Kobayashi, K., Okano, H. and Belluzzi, O. (2005). Functional properties of dopaminergic neurons in the mouse olfactory bulb. *J. Physiol., 564*, 501-514.

Pinching, A.J. and Powell, T.P. (1971a). The neuron types of the glomerular layer of the olfactory bulb. *J. Cell Sci., 9*, 305-345.

Pinching, A.J. and Powell, T.P. (1971b). The neuropil of the glomeruli of the olfactory bulb. *J. Cell Sci., 9*, 347-377.

Pinching, A.J. and Powell, T.P. (1971c). The neuropil of the periglomerular region of the olfactory bulb. *J. Cell Sci., 9*, 379-409.

Pinching, A.J. and Powell, T.P. (1972a). A study of terminal degeneration in the olfactory bulb of the rat. *J. Cell Sci.,10*, 585-619.

Pinching, A.J. and Powell, T.P. (1972b). Experimental studies on the axons intrinsic to the glomerular layer of the olfactory bulb. *J. Cell Sci., 10*, 637-655.

Pinching, A.J. and Powell, T.P. (1972c). The termination of centrifugal fibers in the glomerular layer of the olfactory bulb. *J. Cell Sci., 10*, 621-635.

Potter, S.M., Zheng, C., Koos, D.S., Feinstein, P., Fraser, S.E. and Mombaerts, P. (2001). Structure and emergence of specific olfactory glomeruli in the mouse. *J. Neurosci., 21*, 9713-9723.

Pow, D.V., Sullivan, R., Reye, P. and Hermanussen, S. (2002). Localization of taurine transporters, taurine, and 3H taurine accumulation in the rat retina, pituitary, and brain. *Glia, 37*, 153–168.

Price, J.L. and Powell, T.P.S. (1970a). An electron-microscopic study of the termination of the afferent fibers to the olfactory bulb from the cerebral hemisphere. *J. Cell Sci., 7*, 157–187.

Price, J.L. and Powell, T.P.S. (1970b). The morphology of the granule cells of the olfactory bulb. *J. Cell. Sci., 9*, 91-123.

Puopolo, M. and Belluzzi, O. (1996). Sodium current in periglomerular cells of rat olfactory bulb *in vitro*. *Neuroreport, 7*, 1846-1850.

Puopolo, M. and Belluzzi, O. (1998). Functional heterogeneity of periglomerular cells in the rat olfactory bulb. *Eur. J. Neurosci., 10*, 1073-1083.

Ressler, K.J., Sullivan, S.L. and Buck, L.B. (1993). A zonal organization of odorant receptor gene expression in the olfactory epithelium. *Cell, 73*, 597-609.

Ressler, K.J., Sullivan, S.L. and Buck, L.B. (1994). Information coding in the olfactory system: evidence for a stereotyped and highly organized epitope map in the olfactory bulb. *Cell, 79*, 1245-1255.

Ribak, C.E., Vaughn, J.E., Saito, K., Barber, R. and Roberts, E. (1977). Glutamate decarboxylase localization in neurons of the olfactory bulb. *Brain Res., 126*, 1-18.

Ross, C.D., Godfrey, D.A. and Parli, J.A., (1995). Amino acid concentrations and selected enzyme activities in rat auditory, olfactory, and visual systems. *Neurochem. Res., 20*, 1483–1490.

Roy, S.A. and Alloway, K.D. (2001). Coincidence detection or temporal integration? What the neurons in somatosensory cortex are doing. *J. Neurosci., 21*, 2462-2473.

Salin, P.A., Lledo, P.M. Vincent, J.D. and Charpak, S. (2001). Dendritic glutamate autoreceptors modulate signal processing in rat mitral cells. *J. Neurophysiol., 85*, 1275-1282.

Sallaz, M. and Jourdan, F. (1992). Apomorphine disrupts odour-induced patterns of glomerular activation in the olfactory bulb. *NeuroReport, 3*, 833-836.

Sassoe-Pognetto, M., Cantino, D. and Panzanelli, P. (1993). Presynaptic co-localization of carnosine and glutamate in olfactory neurons. *NeuroReport, 5*, 7-10

Schoenfeld, T.A., Marchand, J.E. and Macrides, F. (1985). Topographic organization of tufted cell axonal projections in the hamster main olfactory bulb: an intrabulbar associational system. *J. Comp. Neurol., 235*. 503-518.

Schoppa, N.E., and Urban, N.N. (2003). Dendritic processing within olfactory bulb circuits. *Trends Neurosci., 26*, 501-506.

Schoppa, N.E., Kinzie, J.M., Sahara, Y., Segerson, T.P. and Westbrook, G.L. (1998). Dendrodendritic inhibition in the olfactory bulb is driven by NMDA receptors. *J. Neurosci, 18*, 6790-6802.

Schoppa, N.E. and Westbrook, G.L. (2001). Glomerulus-specific synchronization of mitral cells in the olfactory bulb. *Neuron, 31*, 639-651.

Schoppa, N.E. and Westbrook, G.L. (2002). AMPA receptors drive correlated spiking in olfactory bulb glomeruli. *Nat. Neurosci., 5*, 1194-1202.

Scott J.W. (1981). Electrophysiological identification of mitral and tufted cells and distributions of their axons in olfactory system of the rat. *J. Neurophysiol., 46*, 918-931.

Shepherd, G.M. (1972). Synaptic organization of the mammalian olfactory bulb. *Physiol. Rev., 52*, 864-917.

Shepherd, G.M. and Brayton, R.K. (1979). Computer simulation of a dendrodendritic synaptic circuit for self- and lateral-inhibition in the olfactory bulb. *Brain Res., 175*, 377-382.

Shepherd, G.M., and Greer, C.A. (1998). The olfactory bulb. In G.M. Shepherd (Ed.) *The synaptic organization of the brain* (pp. 159-203). New York, ST: Oxford UP.

Shipley, M.T., McLean, J.H., Zimmer, L.A., and Ennis, M. (1996). The olfactory system. In: *Handbook of chemical neuroanatomy, Vol 12*, Integrated systems of the CNS, Pt III (Björklund, A., Hökfelt, T., Swanson, L.W., eds), pp 469-573. Amsterdam: Elsevier.

Siklos, L., Rickmann, M., Joo, F., Freeman, W.J. and Wolff, J.R. (1995). Chloride is preferentially accumulated in a subpopulation of dendrites and periglomerular cells of the main olfactory bulb in adult rats. *Neurosci., 64*, 165-172.

Smith, T.C. and Jahr, C.E. (2002). Self-inhibition of olfactory bulb neurons. *Nat. Neurosci., 5*, 760-6.

Spors, H., Wachowiak, M., Cohen, L.B., and Friedrich, R.W. (2005). Temporal dynamics and latency patterns of receptor neuron input to the olfactory bulb. *J. Neurosci. 26(4)*, 1247-59.

Stopfer, M., Bhagavan, S., Smith, B.H., and Laurent, G. (1997). Impaired odour discrimination on desynchronization of odour-encoding neural assemblies. *Nature, 390*, 70-74.

Storch, A., Lester, H.A., Boehm, B.O., and Schwarz, J. (2003). Functional characterization of dopaminergic neurons derived from rodent mesencephalic progenitor cells. *J. Chem. Neuroanat., 26(2)*, 133-42.

Su, H., Alroy, G., Kirson, E.D., and Yaari, Y. (2001) Extracellular calcium modulates persistent sodium current-dependent burst-firing in hippocampal pyramidal neurons. *J. Neurosci.*, 21, 4173-4182.

Toida, K., Kosaka, K., Aika, Y. and Kosaka, T. (2000). Chemically defined neuron groups and their subpopulations in the glomerular layer of the rat main olfactory bulb--IV.

Intraglomerular synapses of tyrosine hydroxylase-immunoreactive neurons. *Neurosci., 101*, 11-17.

Toida, K., Kosaka, K., Heizmann, C.W. and Kosaka, T. (1998). Chemically defined neuron groups and their subpopulations in the glomerular layer of the rat main olfactory bulb: III. Structural features of calbindin D28K-immunoreactive neurons. *J. Comp. Neurol., 392*, 179-198.

Treloar, H.B., Feinstein, P., Mombaerts P. and Greer, C.A. (2002). Specificity of glomerular targeting by olfactory sensory axons. *J. Neurosci., 22*, 2469-2477.

Uchida, N., and Mainen, Z.F. (2003). Speed and accuracy of olfactory discrimination in the rat. *Nat. Neurosci., 6*, 1224-1229.

Urban, N.N. and Sakmann, B. (2002). Reciprocal intraglomerular excitation and intra- and interglomerular lateral inhibition between mouse olfactory bulb mitral cells. *J. Physiol. (Lond), 542*, 355–367.

Van Gehuchten, L.E. and Martin, A. (1891). Le bulbe olfactif chez quelques mammiferes. *Cellule,* 205-237.

Vassar, R., Chao, S.K., Sitcheran, R., Nunez, J.M., Vosshall, L.B. and Axel, R. (1994). Topographic organization of sensory projections to the olfactory bulb. *Cell, 79*, 981-991.

Vnek, N., Ramsden, B.M., Hung, C.P., Goldman-Rakic, P.S., and Roe, A.W. (1999). Optical imaging of functional domains in the cortex of the awake and behaving monkey. *Proc. Natl. Acad. Sci. USA, 96*, 4057-4060.

Wachowiak, M. and Cohen, L.B. (1999). Presynaptic inhibition of primary olfactory afferents mediated by different mechanisms in lobster and turtle. *J. Neurosci., 19*, 8808-8817.

Wachowiak, M., McGann, J.P., Heyward, P.M., Shao, Z., Puche, A.C. and Shipley, M.T. (2005). Inhibition [corrected] of olfactory receptor neuron input to olfactory bulb glomeruli mediated by suppression of presynaptic calcium influx. *J. Neurophysiol., 94*, 2700-2712.

Wang, F., Nemes, A., Mendelsohn, M. and Axel, R. (1998). Odorant receptors govern the formation of a precise topographic map. *Cell, 93*, 47-60.

Wang, D.D., Krueger, D.D., and Bordey, A. (2003). Biophysical properties and ionic signature of neuronal progenitors of the postnatal subventricular zone in situ. *J. Neurophysiol., 90(4)*, 2291-302.

Wehr, M. and Laurent, G. (1996). Odour encoding by temporal sequences of firing in oscillating neural assemblies. *Nature, 384*, 162-166.

Welker, W.I. (1964). Analysis of sniffing of the albino rat. *Behavior, 22*, 223-244.

Weller, W.L. (1972). Barrels in somatosensory neocortex of the marsupial Trichosurus vulpecula (brush-tailed possum). *Brain Res.*, *43*, 11-24.

Wellis, D.P., Scott, J.W. and Harrison, T.A. (1989). Discrimination among odorants by single neurons of the rat olfactory bulb. *J. Neurophysiol., 61*, 1161-1177.

Wellis, D.P. and Scott, J.W. (1990). Intracellular responses of identified rat olfactory bulb interneurons to electrical and odor stimulation. *J. Neurophysiol., 64*, 932-947.

Westerlund, U., Moe, M.C., Varghese, M., Berg-Johnsen, J., Ohlsson, M., Langmoen, I.A., and Svensson, M. (2003). Stem cells from the adult human brain develop into functional neurons in culture. *Exp. Cell Res., 289(2)*, 378-83.

Willhite, D.C., Nquven, K.T., Masurkar, A.V., Greer, C.A., Shepherd G.M., and Chen, W.R. (2006). Viral tracing identifies distributed columnar organization in the olfactory bulb. *Proc. Natl. Acad. Sci. USA, 103 (33)*, 12592-12597.

Wilson, D.A. and Sullivan, R.M. (1995). The D2 antagonist spiperone mimics the effects of olfactory deprivation on mitral/tufted cell odor response patterns. *J. Neurosci., 15*, 5574-5581.

Woolsey, T.A. and Van der Loos, H. (1970). The structural organization of layer IV in the somatosensory region (SI) of the mouse cerebral cortex. The description of a cortical field composed of discrete cytoarchitectonic units. *Brain Res. 17*, 205-242.

Yuan, Q. and Knopfel, T. (2006). Olfactory nerve stimulation-evoked mGluR1 slow potentials, oscillations and calcium signaling in mouse olfactory bulb mitral cells. *J. Neurophysiol., 95*, 3097-3104.

Zhou, Z,, Xiong, W., Masurkar, A.V., Chen W.R. and Shepherd, G.M. (2006). Dendritic calcium plateau potential modulate input-output properties of juxstaglomerular cells in the rat olfactory bulb. *J. Neurophysiol.*, in press.